Galactic Foreground in Planck Era and Beyond: Emission and Polarization from Interstellar Dust

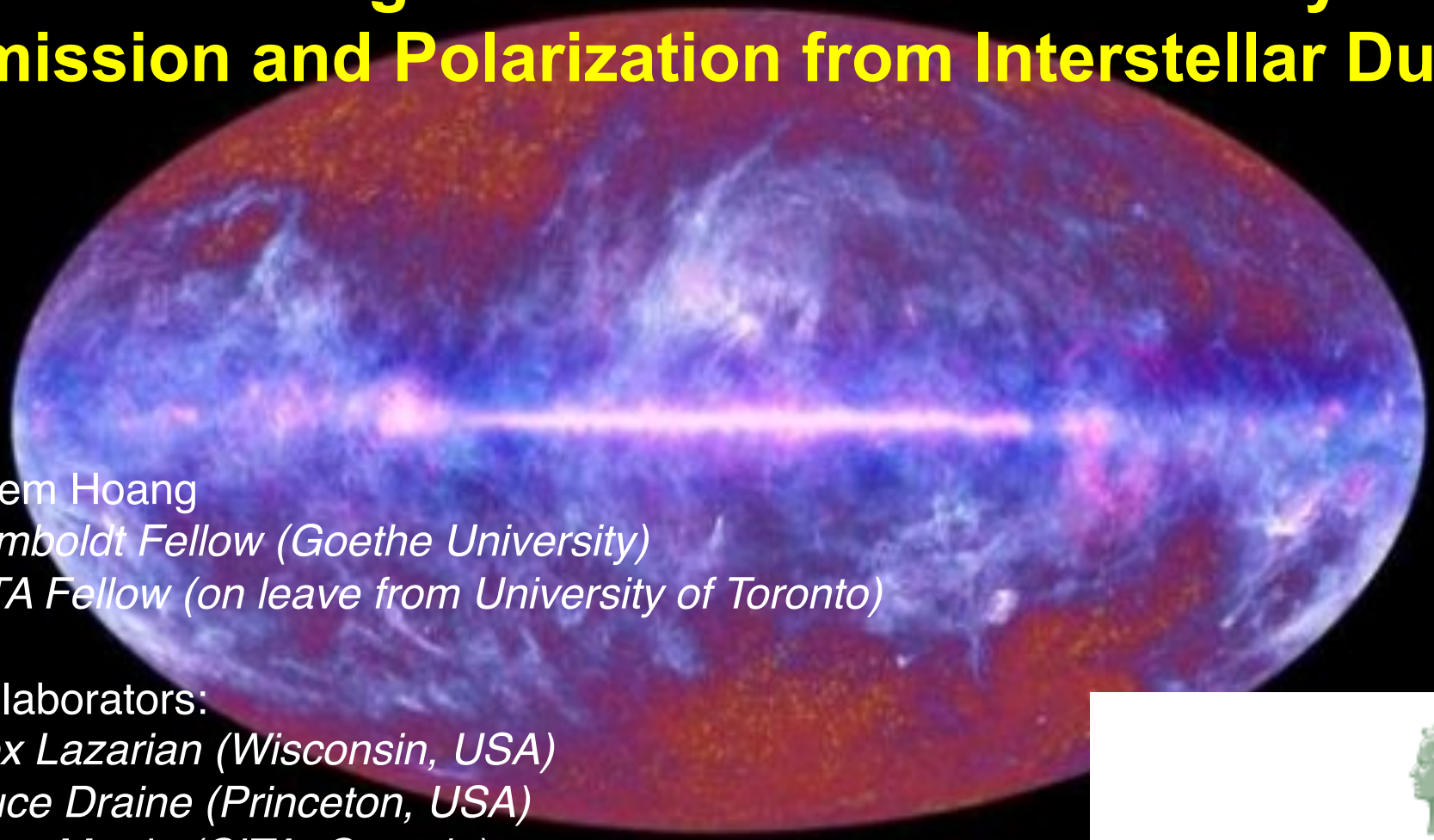

Thiem Hoang
Humboldt Fellow (Goethe University)
CITA Fellow (on leave from University of Toronto)

Collaborators:
Alex Lazarian (Wisconsin, USA)
Bruce Draine (Princeton, USA)
Peter Martin (CITA, Canada)
B-G Andersson (NASA)

Alexander von Humboldt
Stiftung/Foundation

The Planck one-year all-sky survey

esa

Outline

- Introduction to Foreground and Motivation
- New Emissions of Galactic Foreground:
  - Spinning Dust Emission
  - Magnetic Dust Emission
- Polarization of Galactic Foreground:
  - Predictive Model of Grain Alignment
  - Modeling Polarization vs. Observations
  - Inversion Problem
- Summary


Dusty Foreground
Background

Galactic Dust

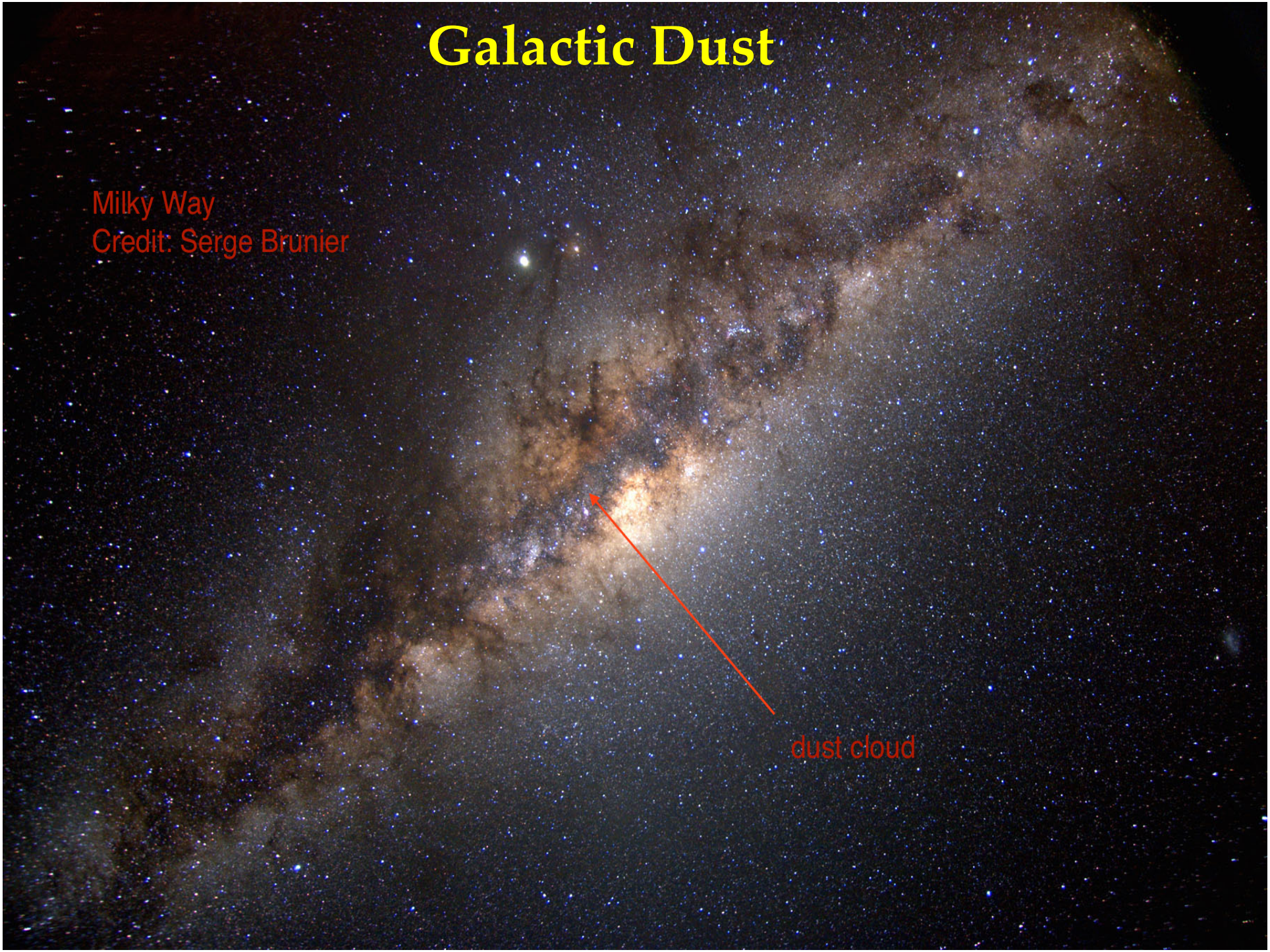

Cosmic Microwave Background (CMB)

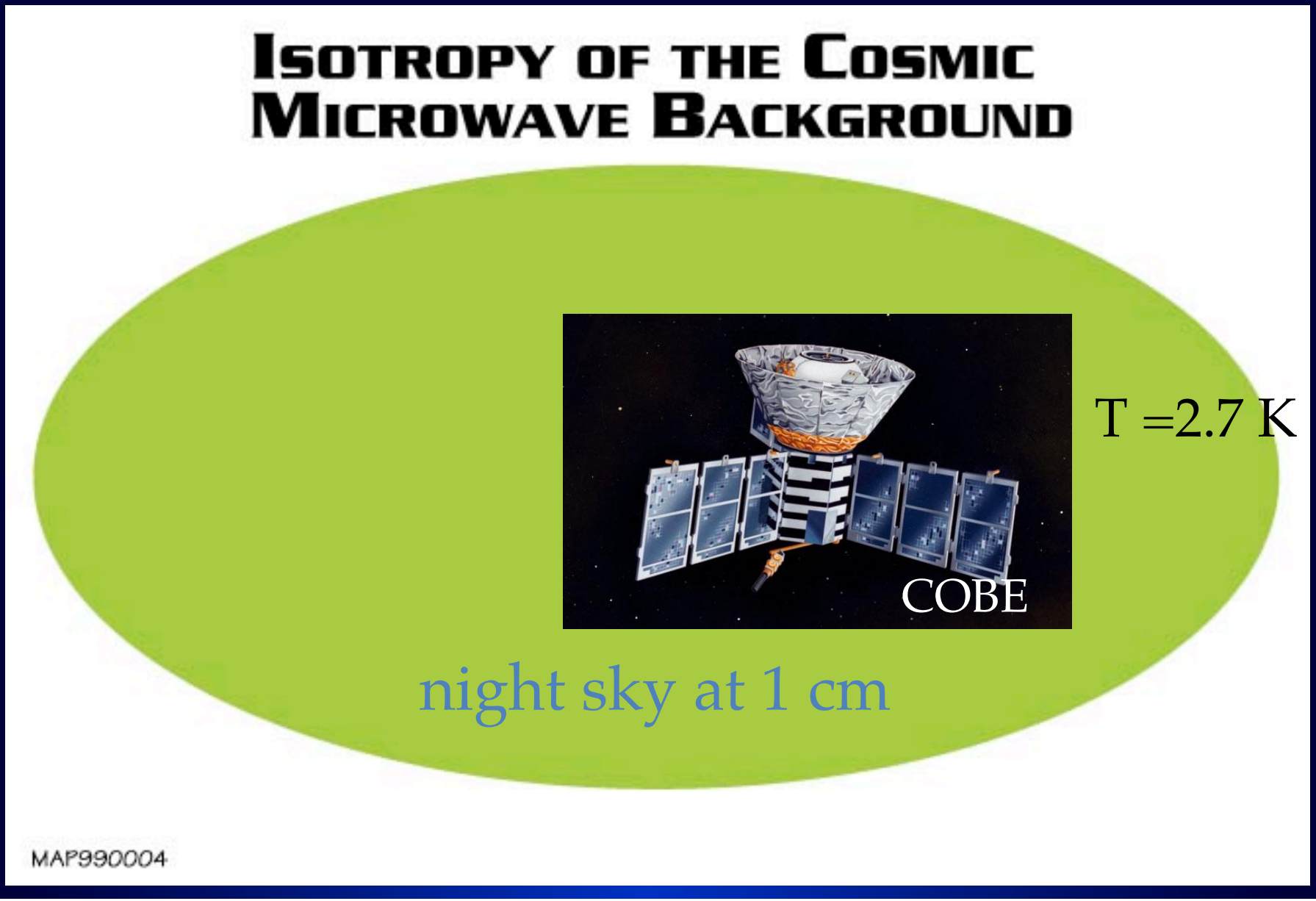

Precision Cosmology

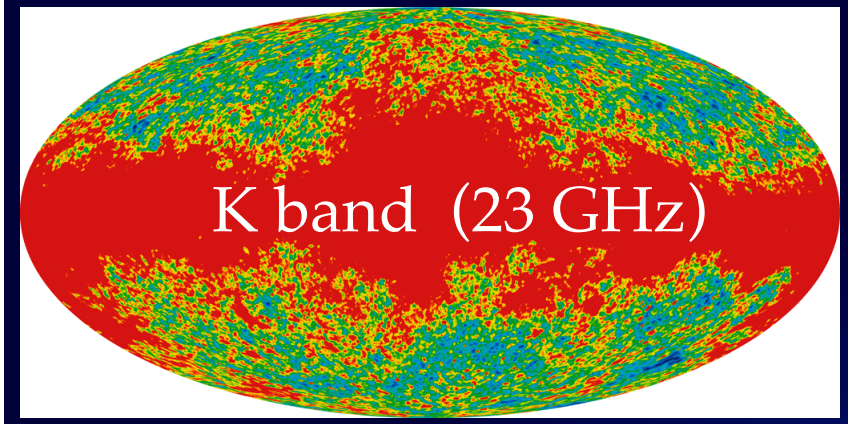

LAMBDA

cleaning

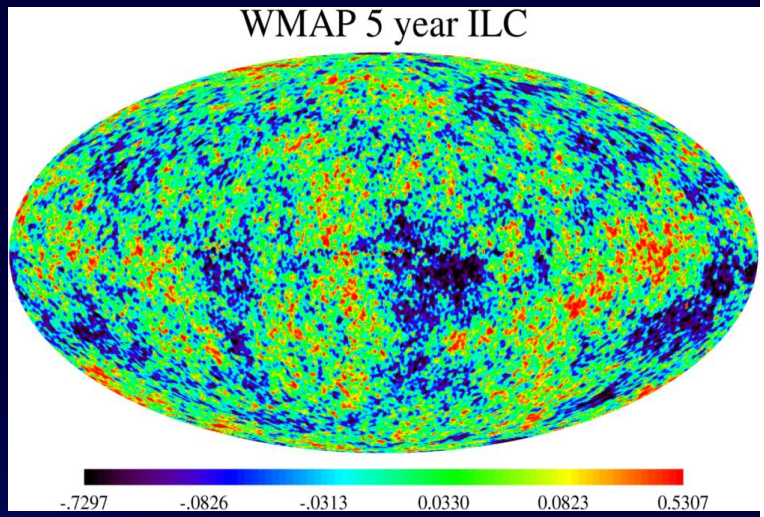

Understanding

Galactic Foregrounds

WMAP Cosmological Parameters Model: lcdm Data: wmap+sdss	
$10^2\Omega_b h^2$	$2.230^{+0.071}_{-0.070}$
$\Delta^2_{\mathcal{R}}(k = 0.002/\mathrm{Mpc})$	$(24.1 \pm 1.3) \times 10^{-10}$
h	0.710 ± 0.026
H_0	71.0 ± 2.6 km/s/Mpc
$n_s(0.002)$	$0.948^{+0.016}_{-0.015}$
$\Omega_b h^2$	$0.02230^{+0.00071}_{-0.00070}$
Ω_Λ	0.735 ± 0.030
Ω_m	0.265 ± 0.030
$\Omega_m h^2$	$0.1327^{+0.0063}_{-0.0064}$

Spergel et al. 2003

WMAP: Wilkinson Microwave Anisotropy Probe

Galactic Foreground Emission

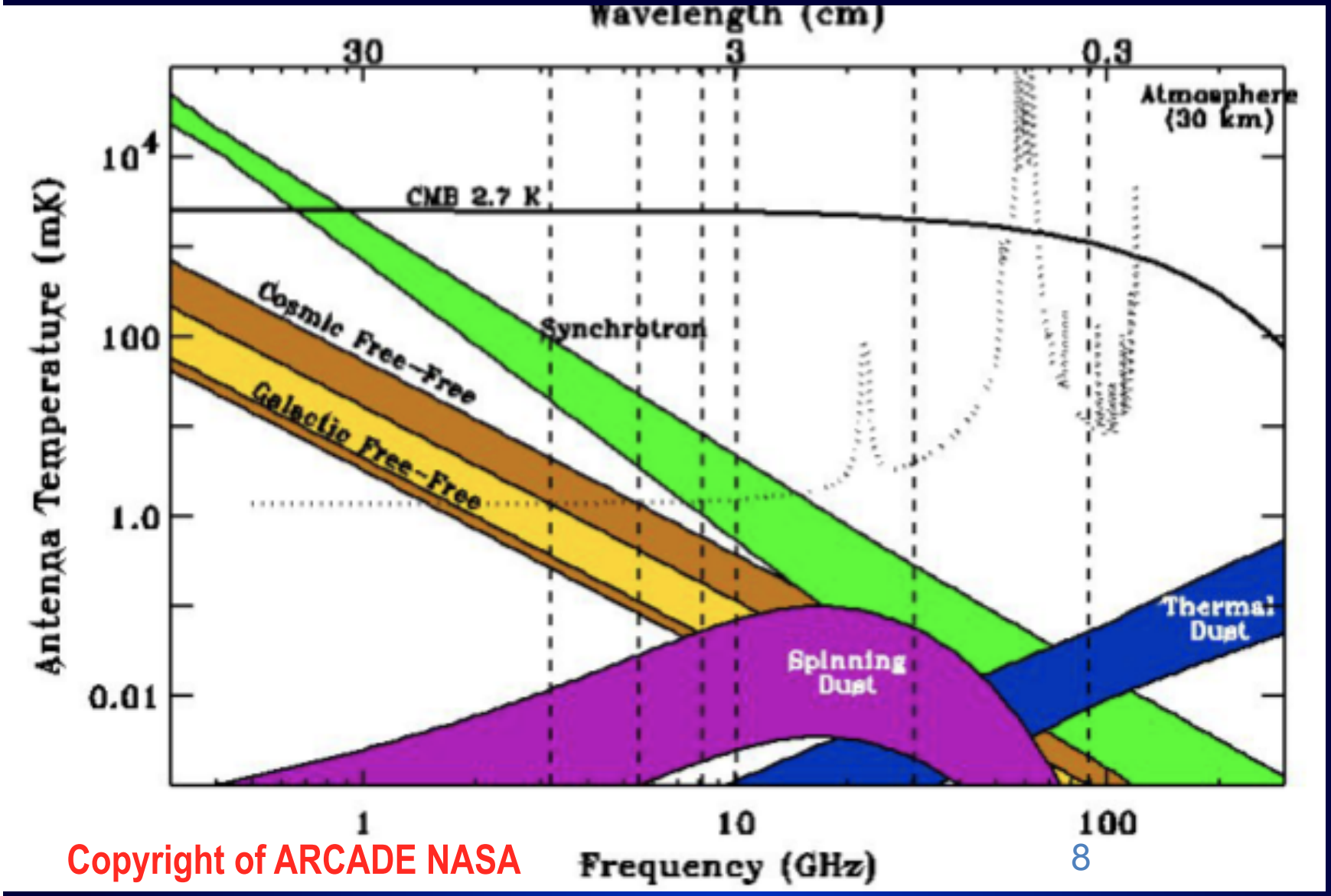

1996: Discovery of anomalous emission by COBE

- Kogut et al. (1996): dust-correlated emission excess at 31 GHz.
- Leitch et al. (1997):
  - *emission excess at 14.5 and 31 GHz*
  - Free-free emission from gas $T \geq 10^6$ K?
- Draine & Lazarian 1998:
  - cannot be free-free emission from 10^6 K gas
  - electric dipole radiation of small dust grains

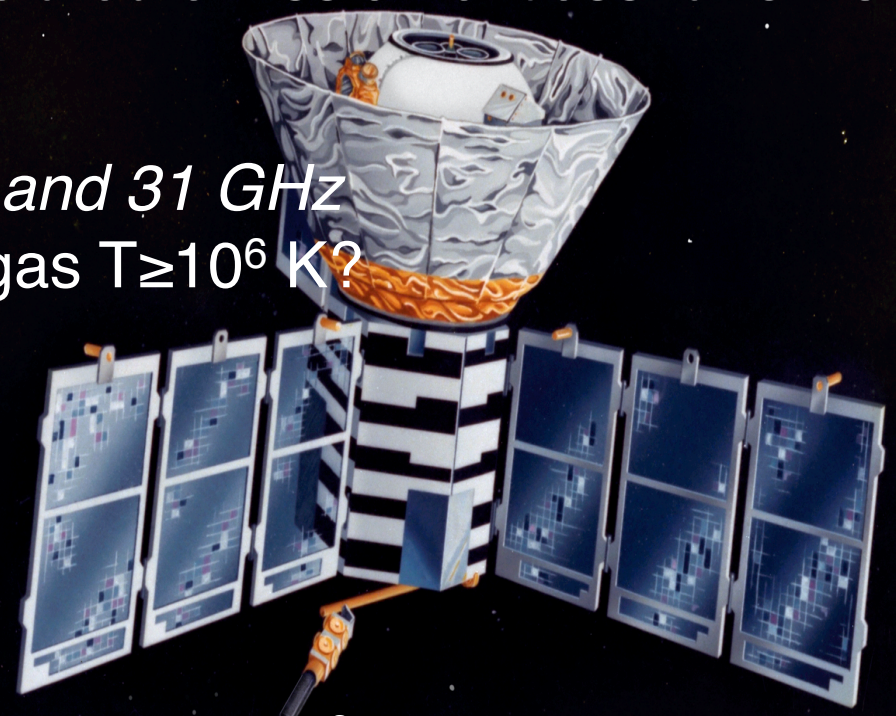

COBE (1989)

Past: Ideas of spinning dust emission can be traced through decades of astrophysical research

Erickson 1957

Ginzburg & Eidman 1959

Ferrara & Dettmar 1994

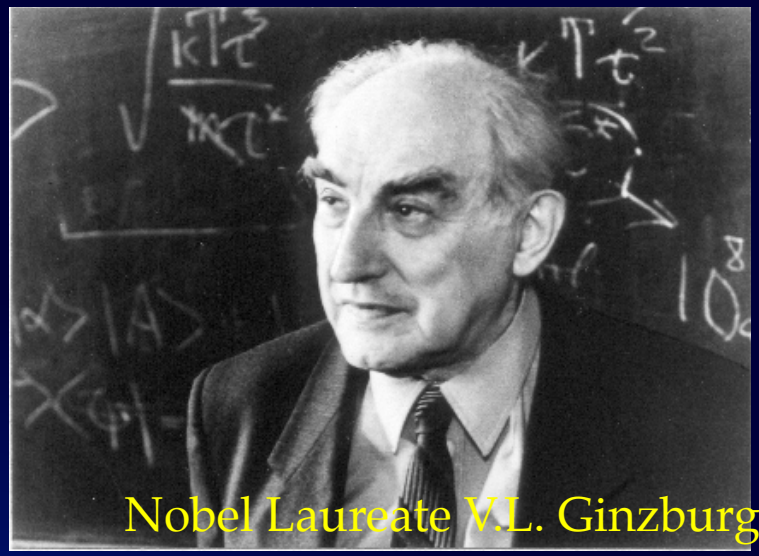

Nobel Laureate V.L. Ginzburg

Two big changes from 50s:

1. Discovery of PAHs (Leger & Puget 1984)
2. Discovery of anomalous emission (Kogut et al. 1996, Leitch et al. 1997)

Small grains are better emitters:

$P \sim \omega^4$ $\omega \sim r^{-5/2}$ $P \sim r^{-10}$

PAH molecules observed in interstellar medium

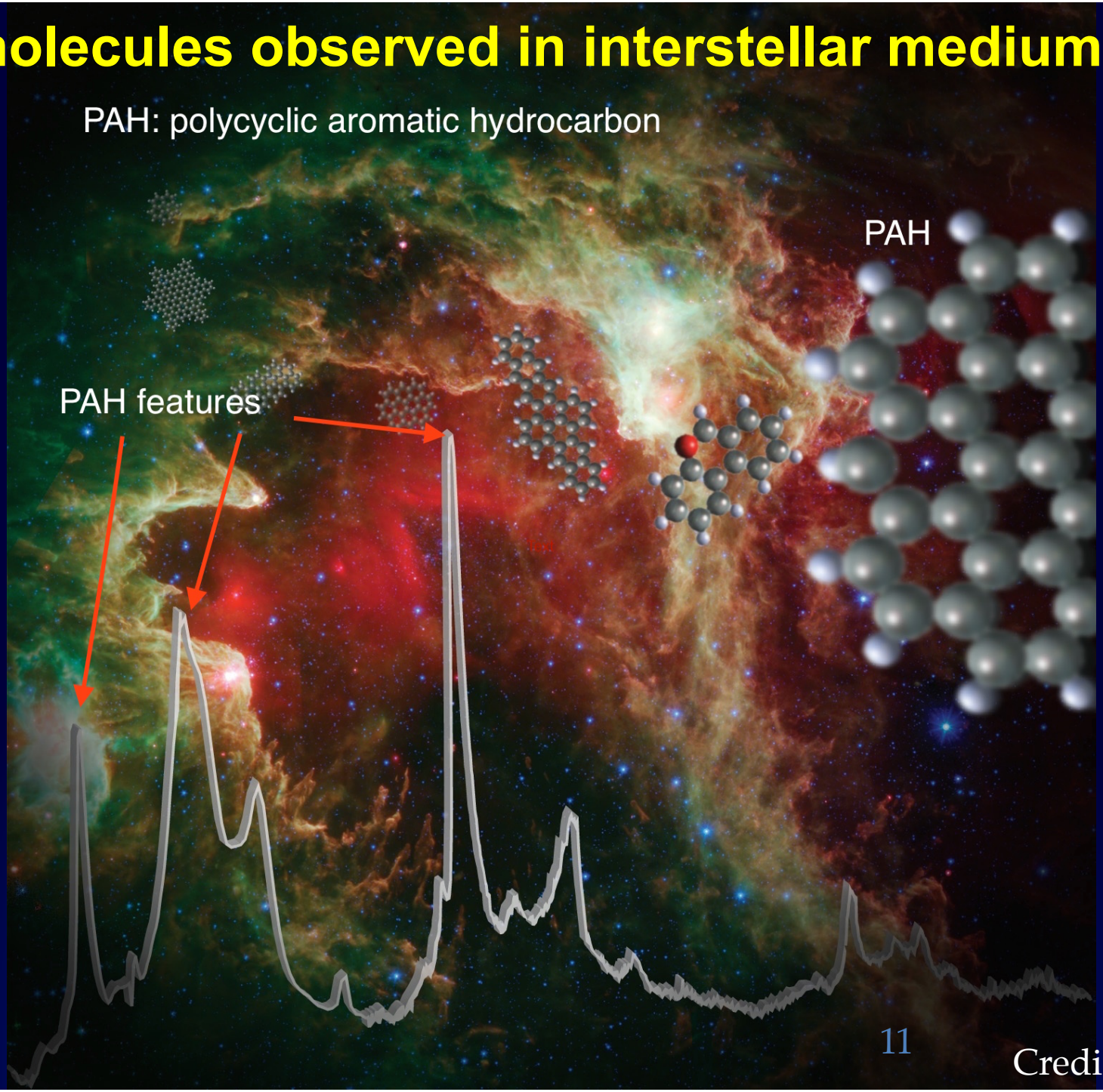

Credit: internet

Electric Dipole Emission from Spinning Dust (Draine & Lazarian 1998)

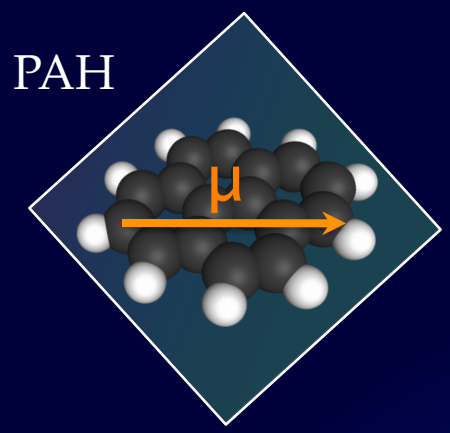

modeling

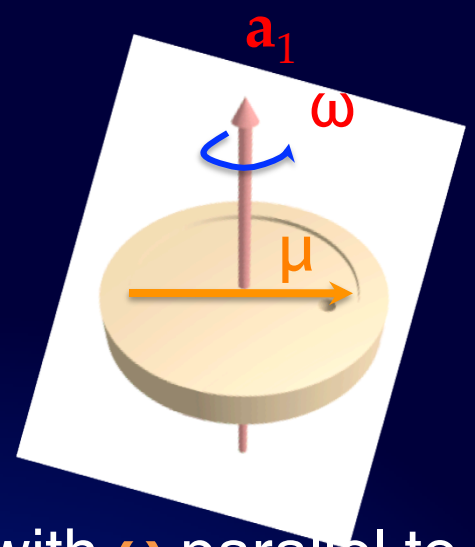

$$\mu = N^{1/2}\beta_0$$

Grain of dipole moment μ, rotating with **ω** parallel to $\mathbf{a}_1$:

- radiates at frequency $\nu = \dfrac{\omega}{2\pi}$
- Emission power: $P_{\mathrm{ed}}(\omega) = \dfrac{2}{3}\dfrac{\mu^2\omega^4}{c^3}$
- Angular velocity distribution: $f_\omega \approx$ *Maxwellian*

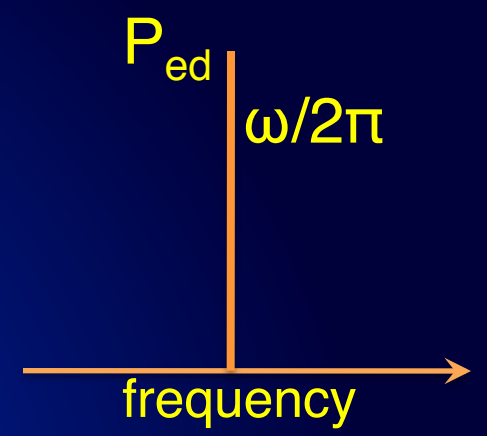

Total emissivity integrated over size distribution *dn/da*:

$$\frac{j_\nu}{n_H} = \frac{1}{4\pi}\int_{a_{\min}}^{a_{\max}} da\,\frac{1}{n_{\mathrm{H}}}\frac{dn}{da}4\pi\omega^2 f_\omega 2\pi P_{\mathrm{ed}}(\omega)$$

$$\left(\mathrm{ergs^{-1}cm^2sr^{-1}Hz^{-1}/H}\right)$$

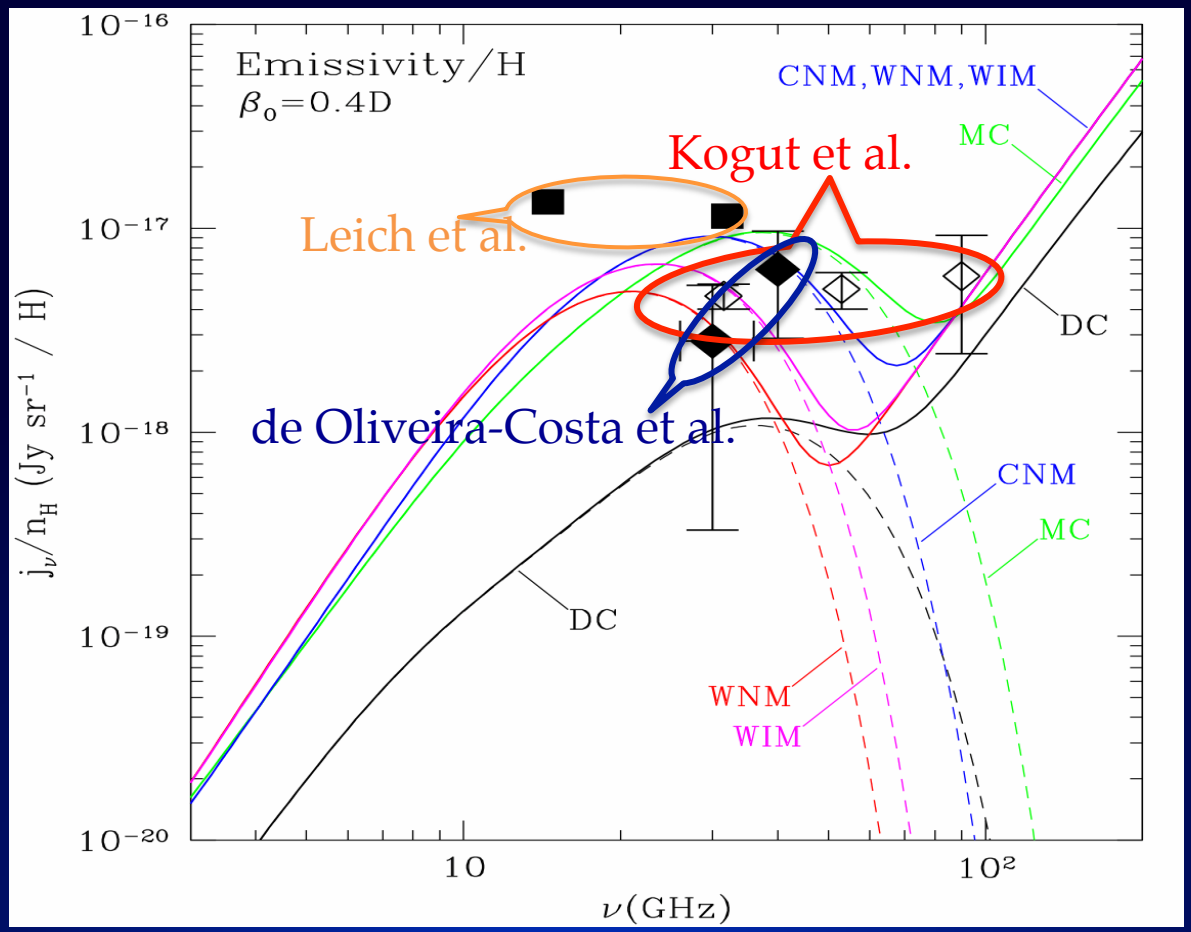

Draine & Lazarian (1998)

DL98 model is supported by numerous observations but requires improvement

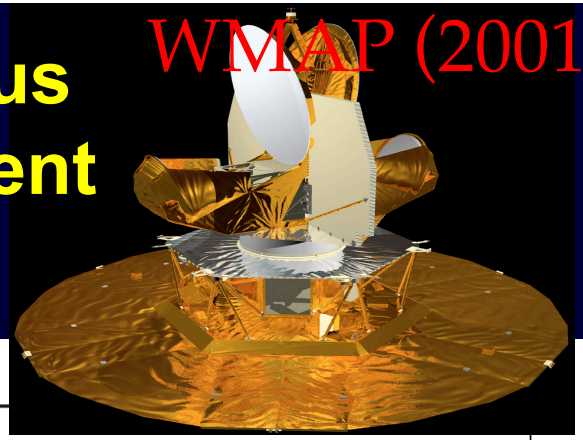

- Five-year WMAP: bump ~ 40 GHz in Hα-correlated spectrum.
- Dobler et al. (2009) adjusted gas density and dipole moment.
- Ali-Haimoud et al. (2009) refined dust-gas interactions.
- Ysard et al. (2010): using quantum method.

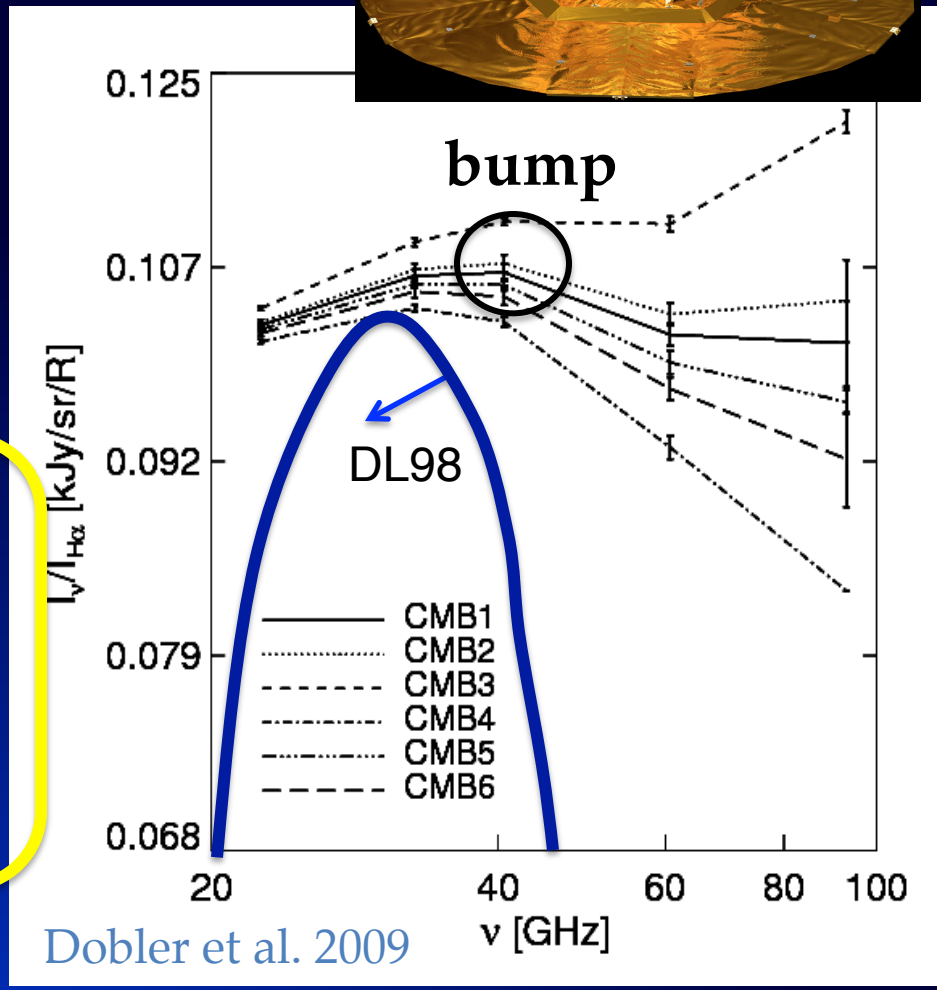

Dobler et al. 2009

Results are not different from the DL98 model.

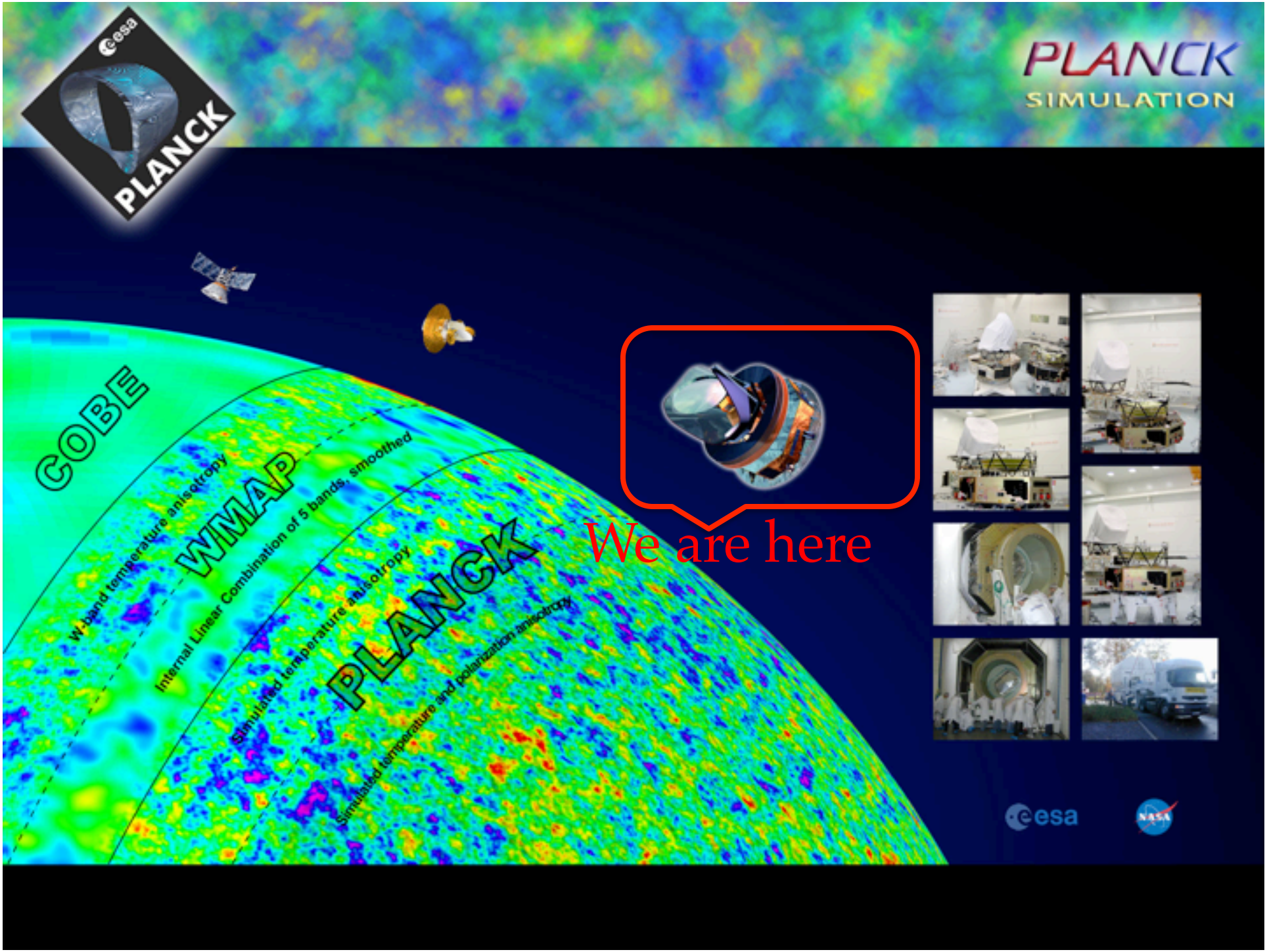
PLANCK
SIMULATION
PLANCK
COBE
W-band temperature anisotropy
WMAP
Internal Linear Combination of 5 bands, smoothed
Simulated temperature anisotropy
PLANCK
Simulated temperature and polarization anisotropy
We are here
esa
NASA

Electric Dipole Emission by Precessing Grain

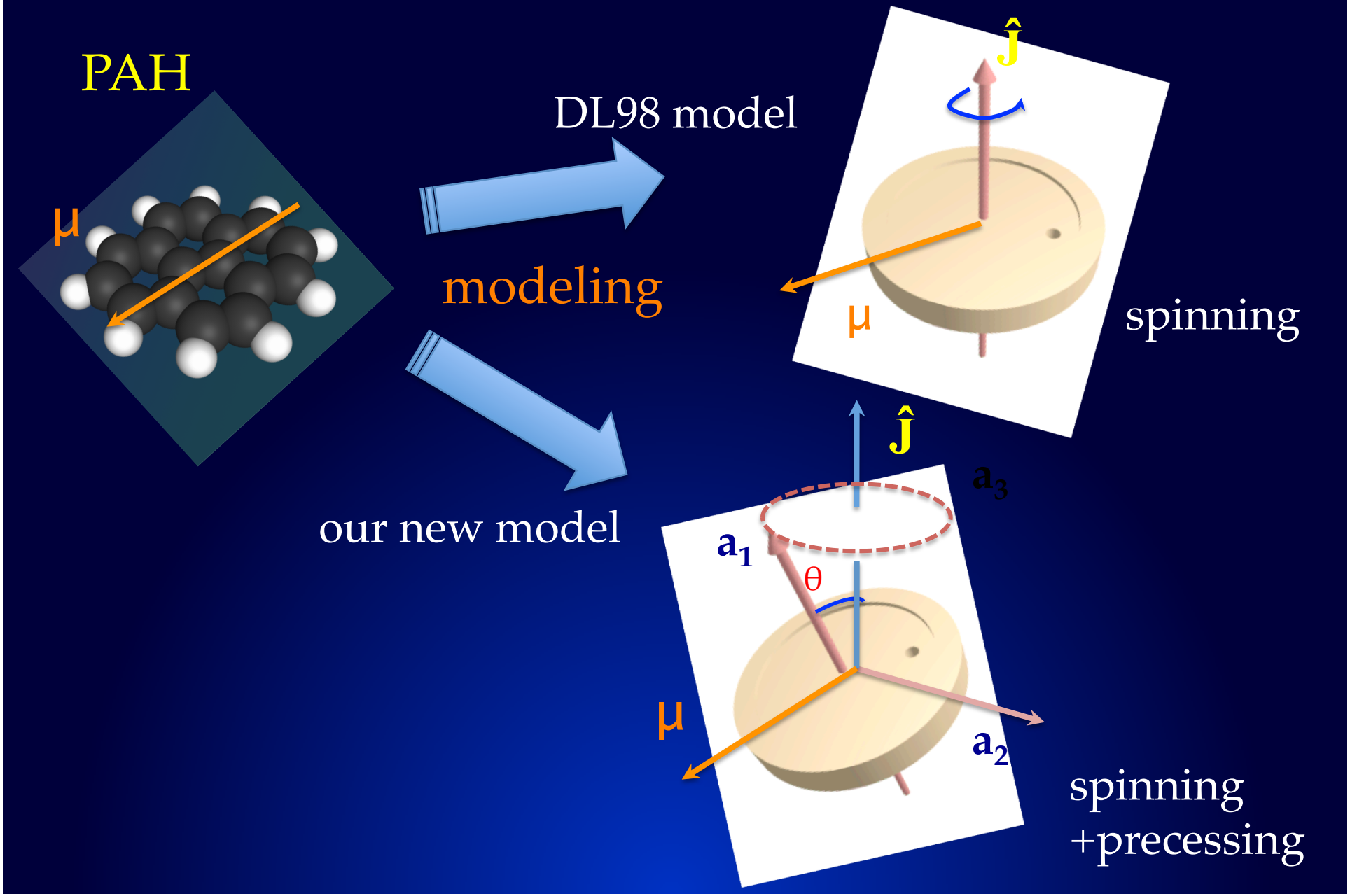

Power Spectrum: Identify Frequency Modes

- Torque-free motion: Euler angles ϕ, ψ, θ, *and* rates

$$\dot{\phi} = \frac{J}{I_2}, \dot{\psi} = \frac{J\cos\theta(1-h)}{I_1}$$

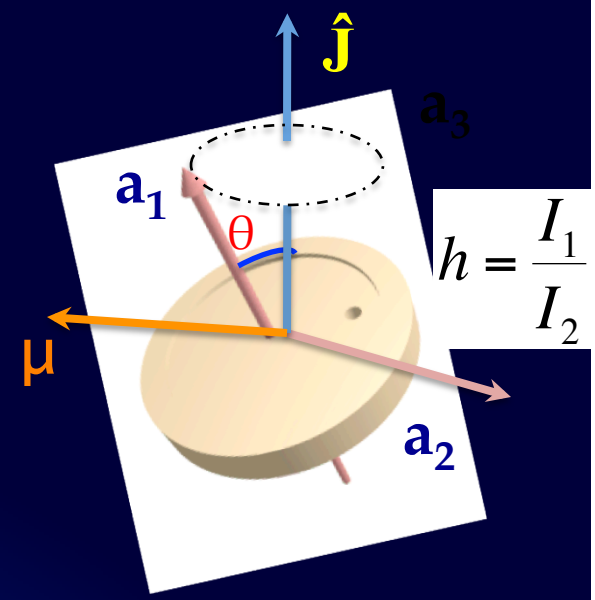

$$h = \frac{I_1}{I_2}$$

- Electric dipole moment: $\mu(J,\theta,t) = \mu_1 a_1 + \mu_2 a_2$
- Fourier Transform: $\ddot{\mu}(J,\theta,t) = \mu_1 \ddot{a}_1 + \mu_2 \ddot{a}_2$

$$\ddot{\mu}_{i,k} = \int_0^\infty \ddot{\mu}_i(t)\exp(-i2\pi\nu_k t)dt,\ i = x,y,z$$

- Power Spectrum:

$$P_{\mathrm{ed},k}(J,\theta) = \frac{2}{3c^3}\sum_i (\ddot{\mu}_{i,k})^2$$

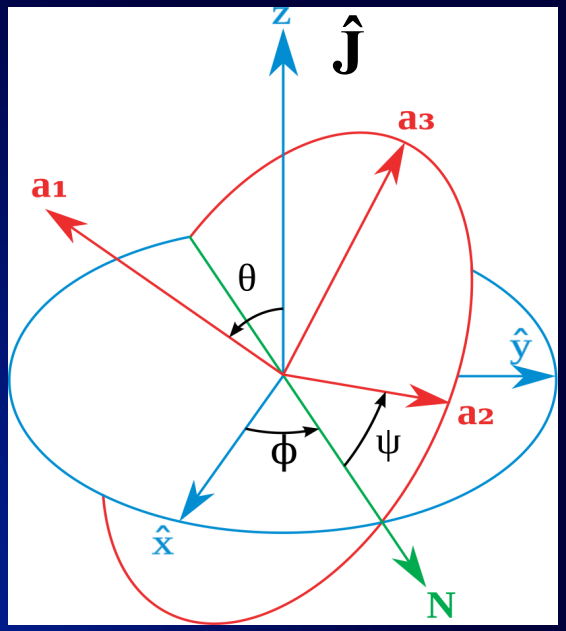

Hoang, Draine & Lazarian 10

Power Spectrum: 4 Frequency Modes

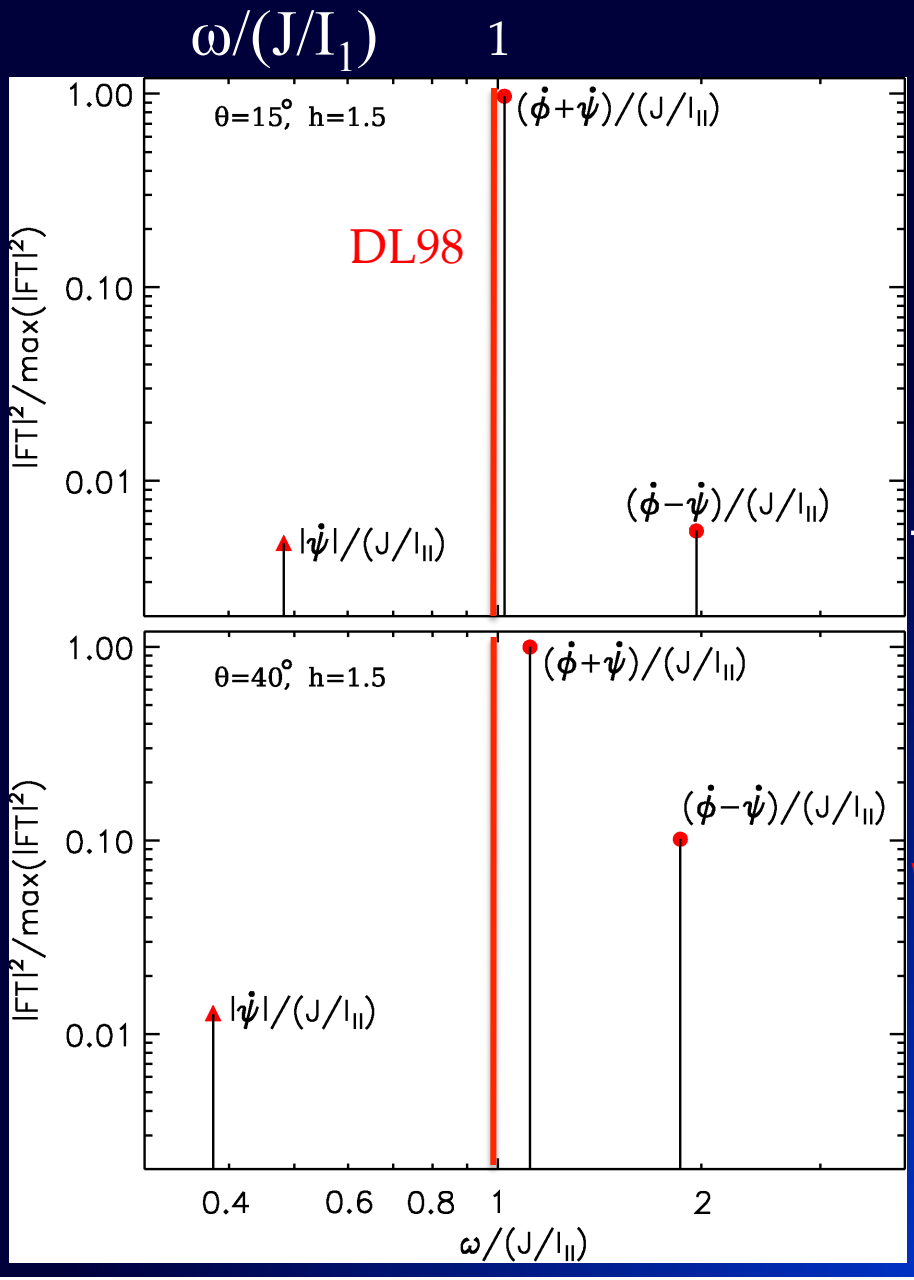

- Precessing grain radiates at frequency modes: $\omega_k = \dot{\phi}, \dot{\phi} \pm \dot{\psi}, \dot{\psi}$
- Dominant modes: $\omega_k = \dot{\phi} \pm \dot{\psi}$

What makes grain rotating?

Hoang, Draine & Lazarian 10

Rotational Damping and Excitation

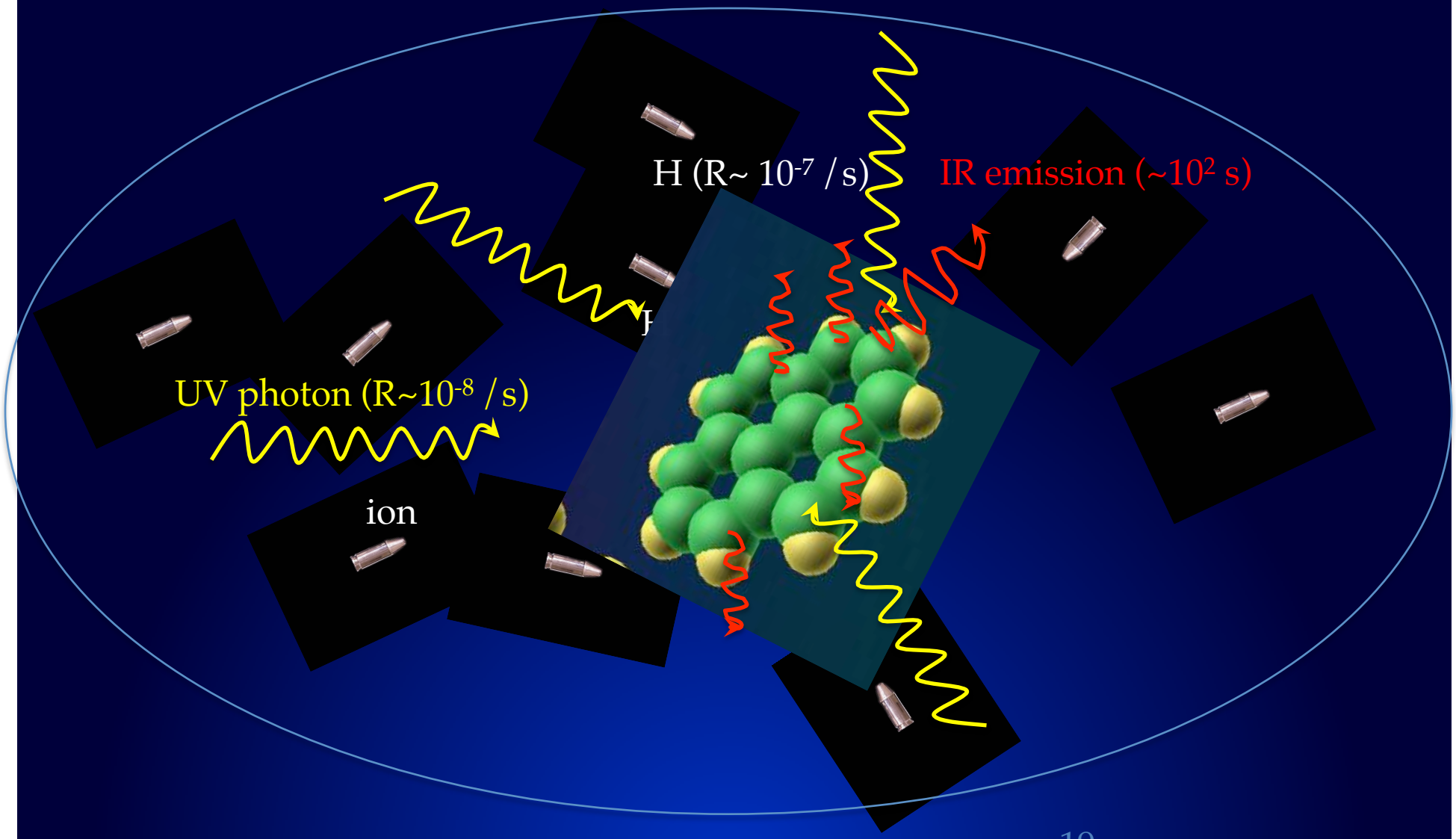

Distribution Function: Solving SDEs

- Angular momentum **J** in the lab system is described by stochastic differential equations (SDEs -Langevin equation):

$$dJ_i = A_i dt + \sqrt{B_{ii}}\, dq_i,\ i = 1,2,3$$

$$A_i = \sum \left\langle \frac{\Delta J_i}{\Delta t} \right\rangle,\ B_{ii} = \sum \left\langle \left(\Delta J_i\right)^2 / \Delta t \right\rangle,\ \left\langle dq^2 \right\rangle = dt$$

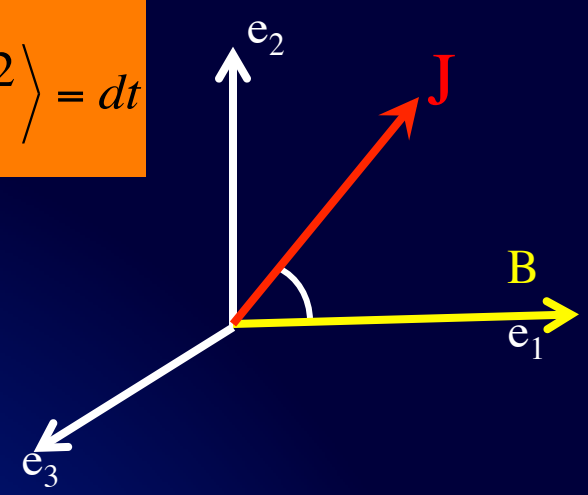

- Damping and excitation coefficients (A_i and B_{ii}) for:
  - dust-neutral and dust-ion collisions
  - infrared emission
  - plasma drag

- Integrate LEs to get J(t) and find momentum distribution f_J
- Emissivity per H atom:

$$\frac{j_\nu}{n_{\mathrm{H}}} = \frac{1}{4\pi}\frac{1}{n_{\mathrm{H}}}\int da \frac{dn}{da} j_\nu^a$$

$$j_\nu^a = \int \mathrm{pdf}(\omega \mid J) P_{\mathrm{ed}}(J) 2\pi f_J dJ$$

Emission Spectrum

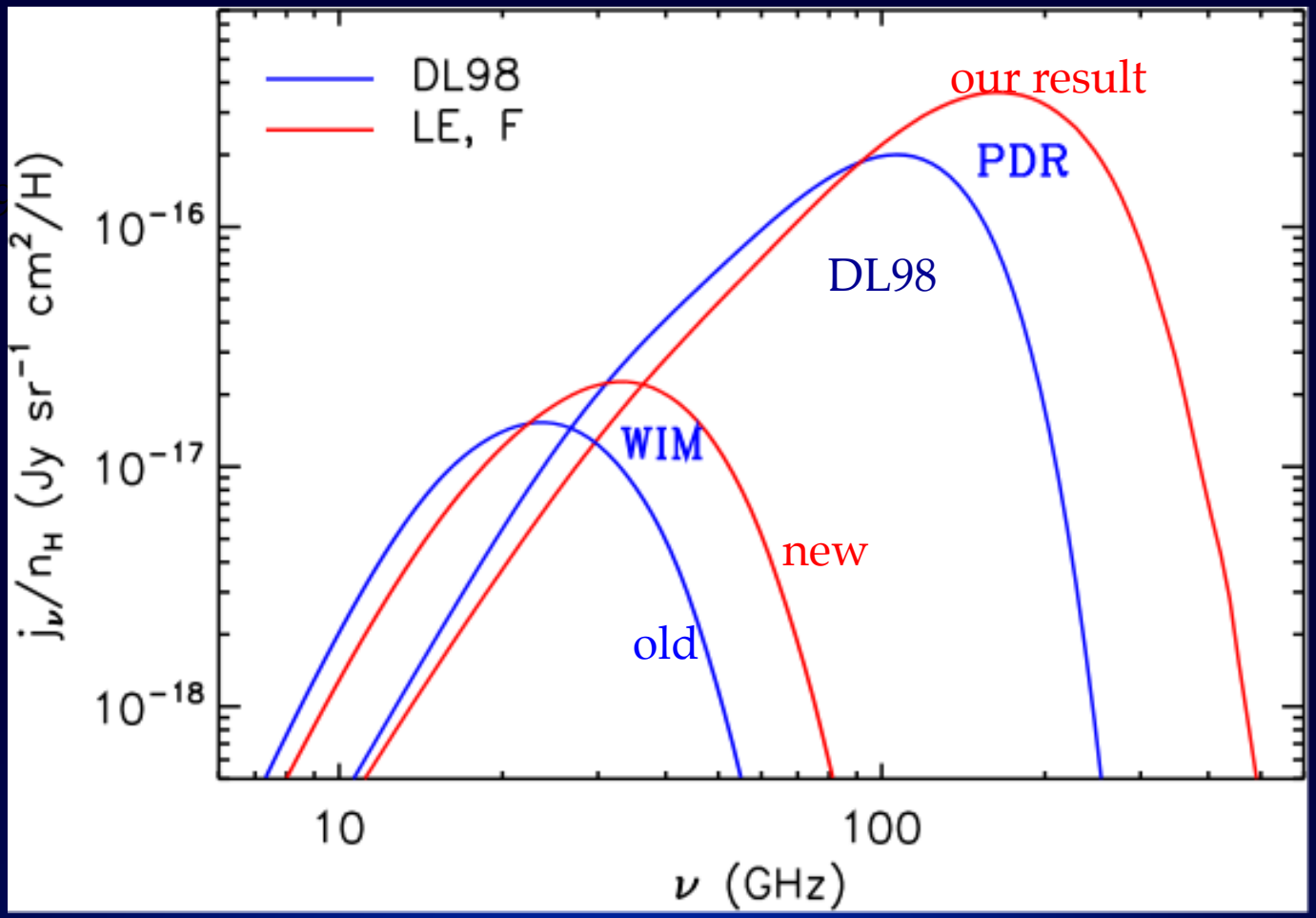

Hoang, Draine & Lazarian 10

- Peak emissivity increases by a factor ~2 .
- Peak frequency increases by factors ~1.4 to 1.8.

Emission from Triaxial PAHs

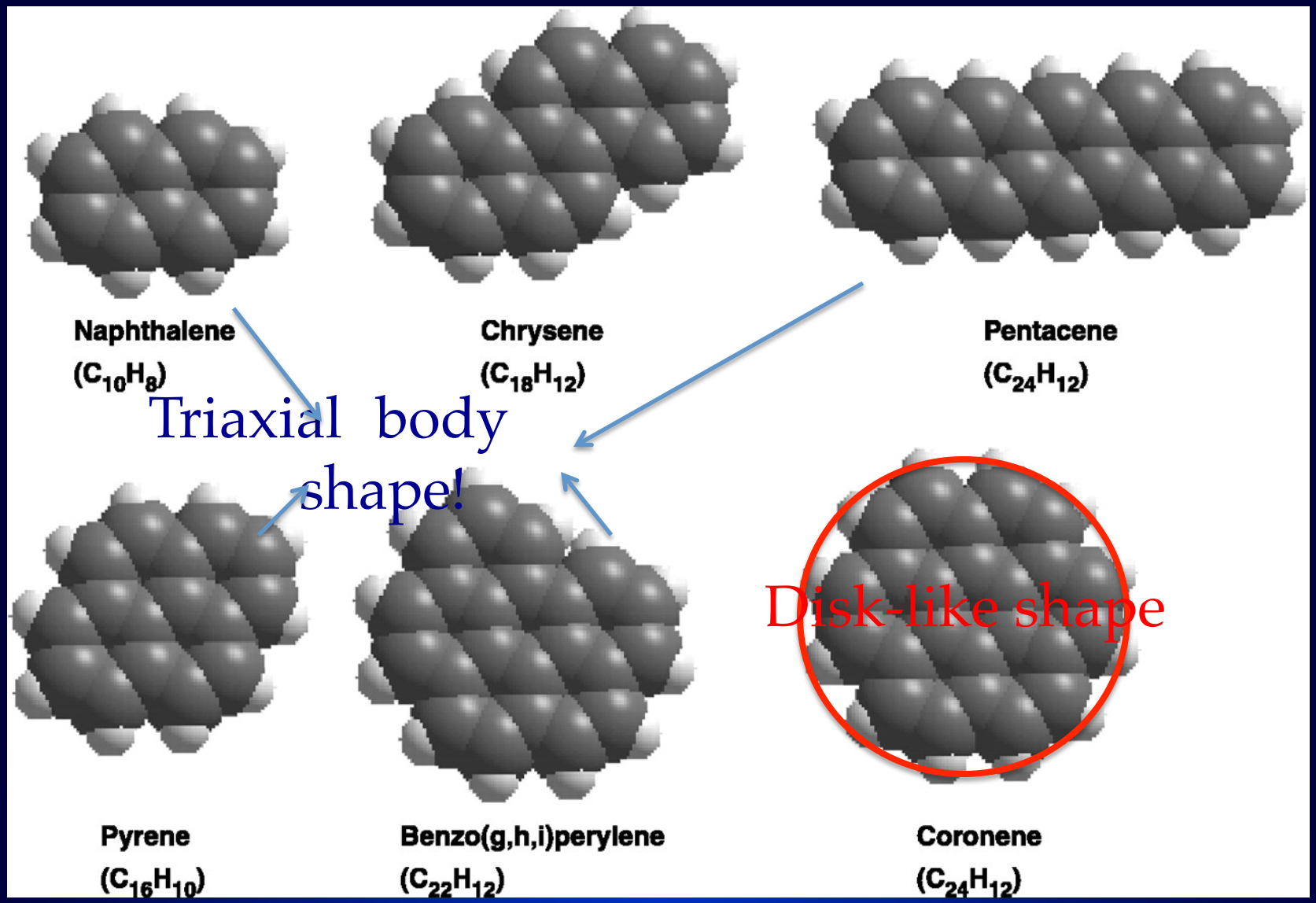

Power Spectrum: Multiple Freq. Modes

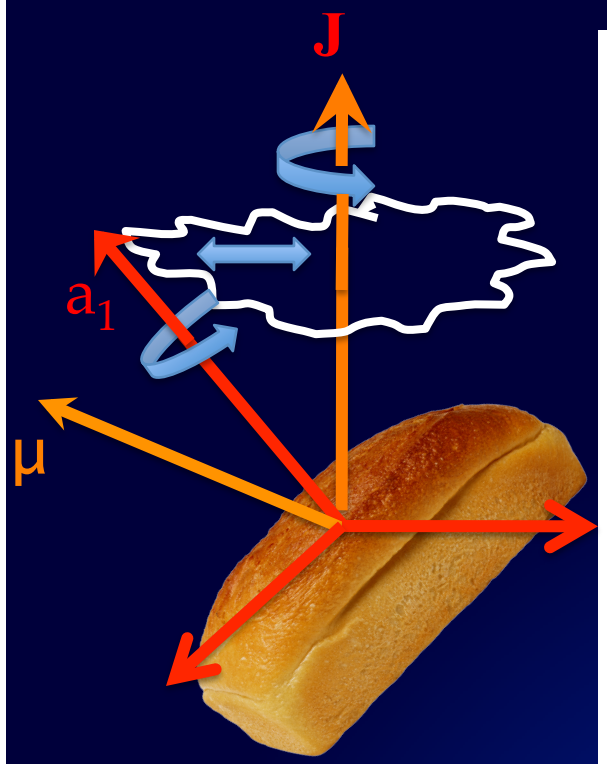

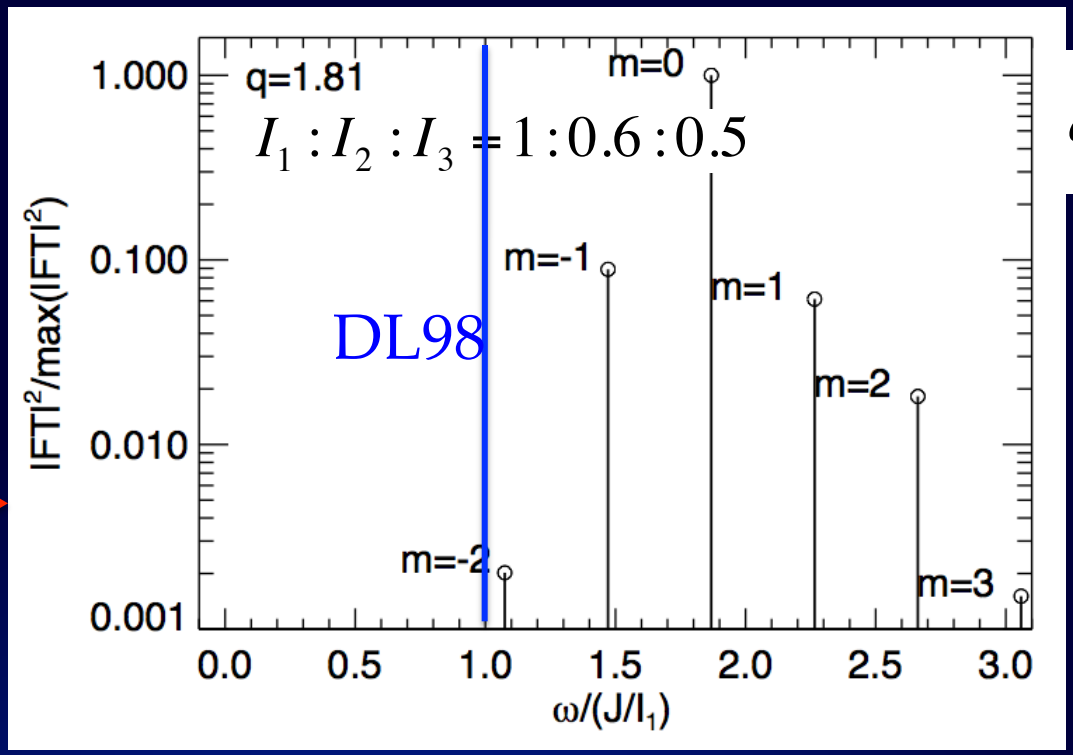

$$q = \frac{2 I_1 E_{\rm rot}}{J^2}$$

- Multiple frequency modes:

$$\omega_m = \langle \dot{\phi} \rangle + m \langle \dot{\psi} \rangle, m = 0, \pm 1, \pm 2 \ldots,$$
$$\omega_n = n \langle \dot{\psi} \rangle, n = 0, 1, 2$$

where <…> denotes time averaging.

Hoang, Lazarian, & Draine 11

Emissivity Increases with Grain Irregularity

- Working model: Simple irregular shape
- Irregularity: $\eta = b_3/b_2$

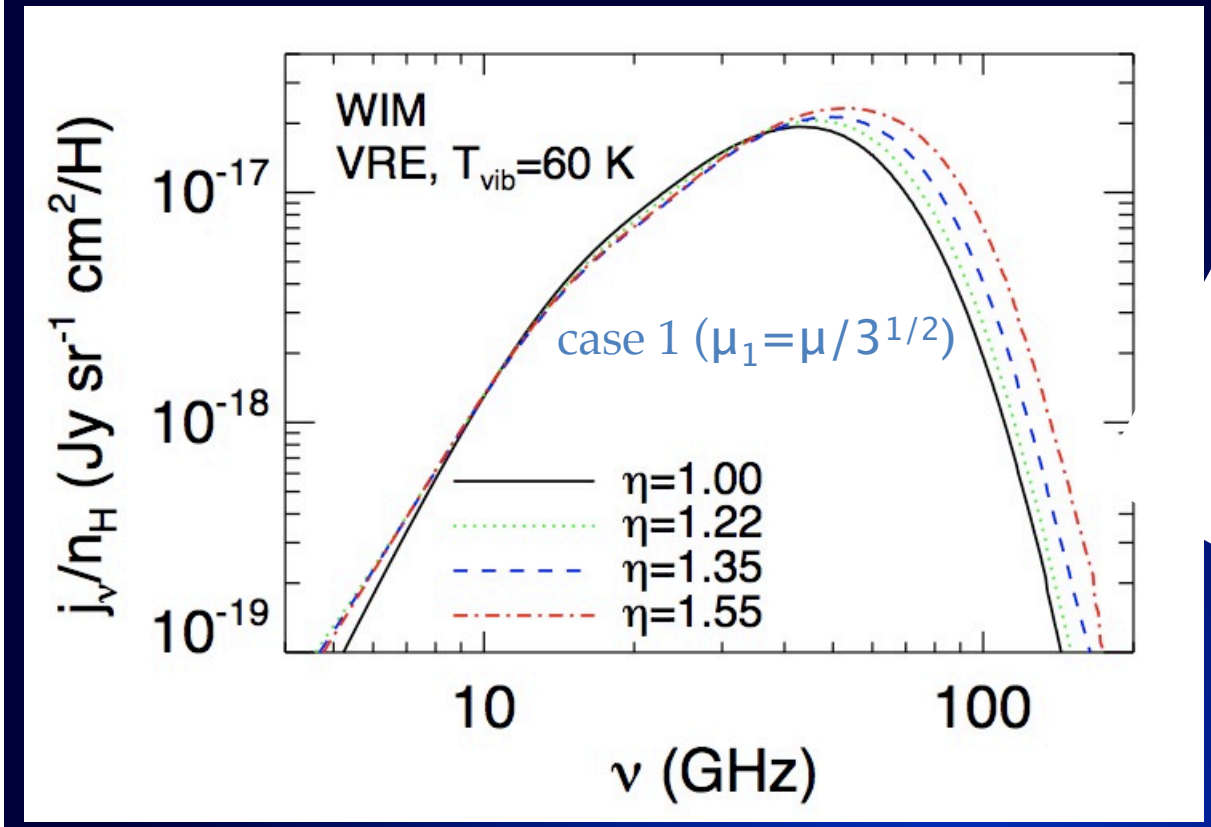

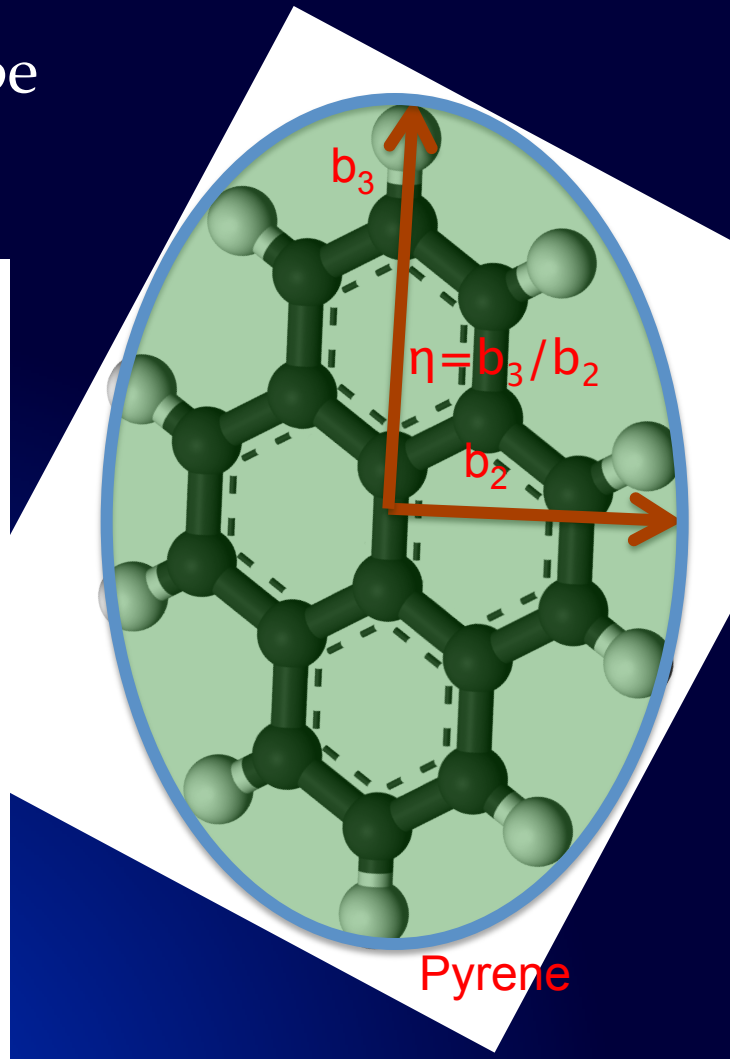

Impulsive excitation by single-ion collisions extends the tail.

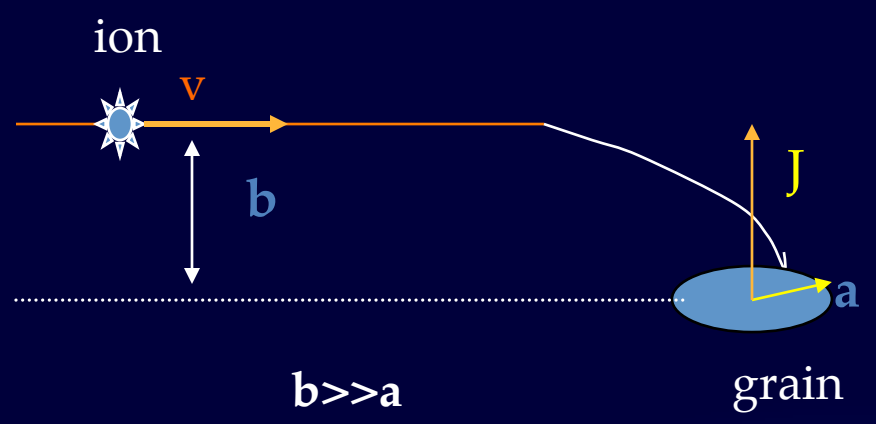

Change in J may be large

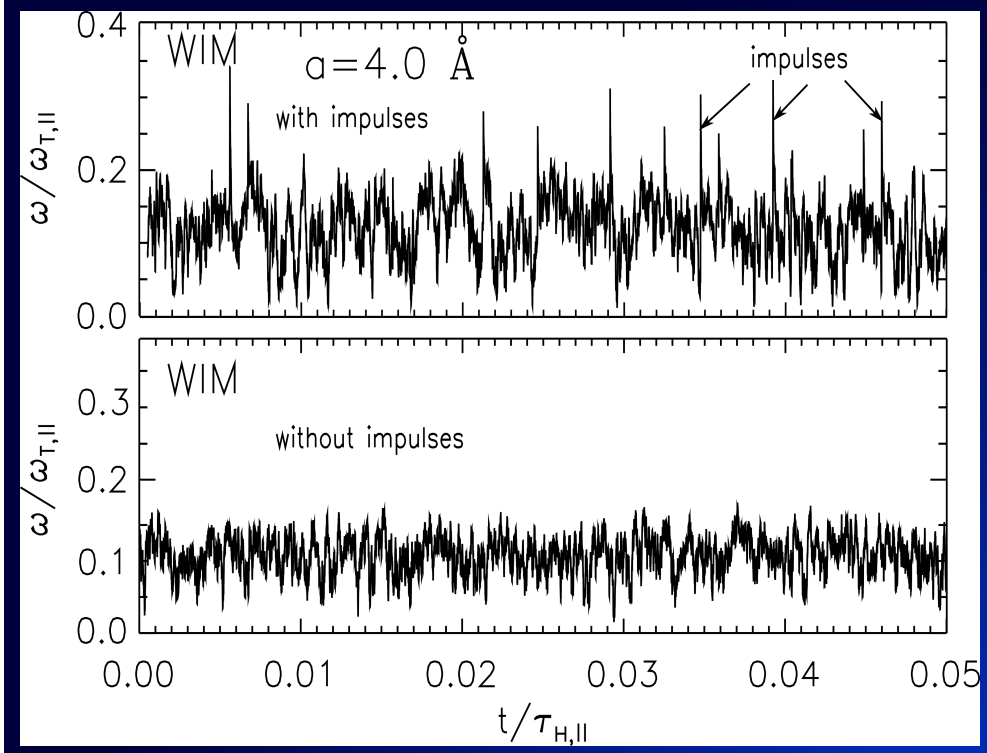

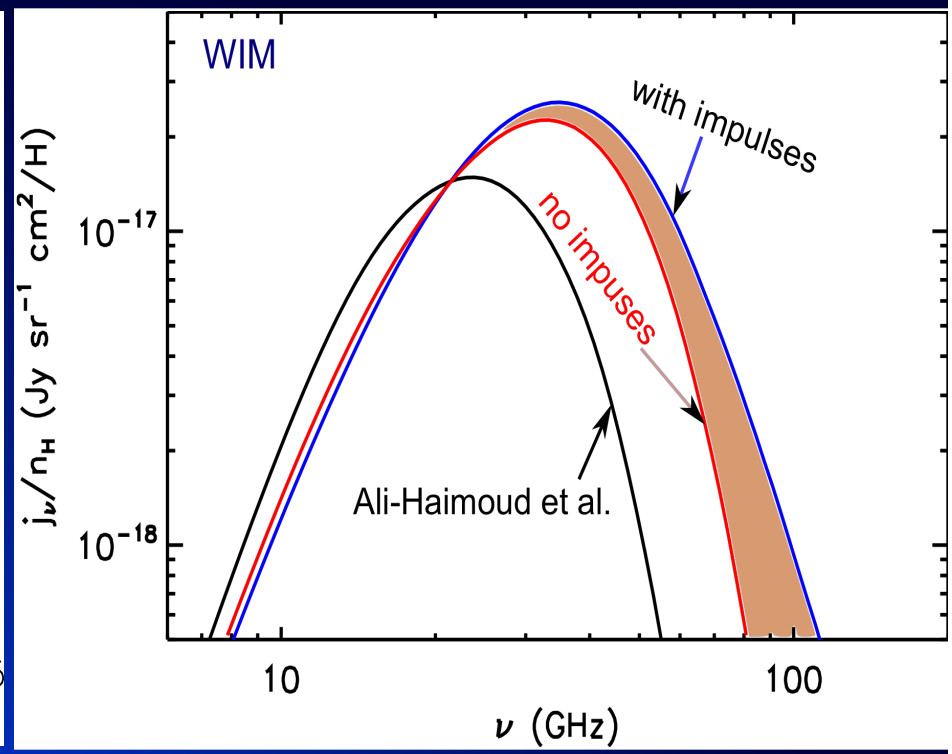

Fitting to WMAP data from H I cloud

$$\frac{I_\nu^{\mathrm{mod}}}{T_{94\mathrm{GHz}}} = Sd_0 \frac{I_\nu^{\mathrm{sd}}(\mathrm{CNM})}{T_{94\mathrm{GHz}}} + C_0\left(\frac{\nu}{23\mathrm{GHz}}\right)^2 + T_0\left(\frac{\nu}{94\mathrm{GHz}}\right)^{3.8}$$

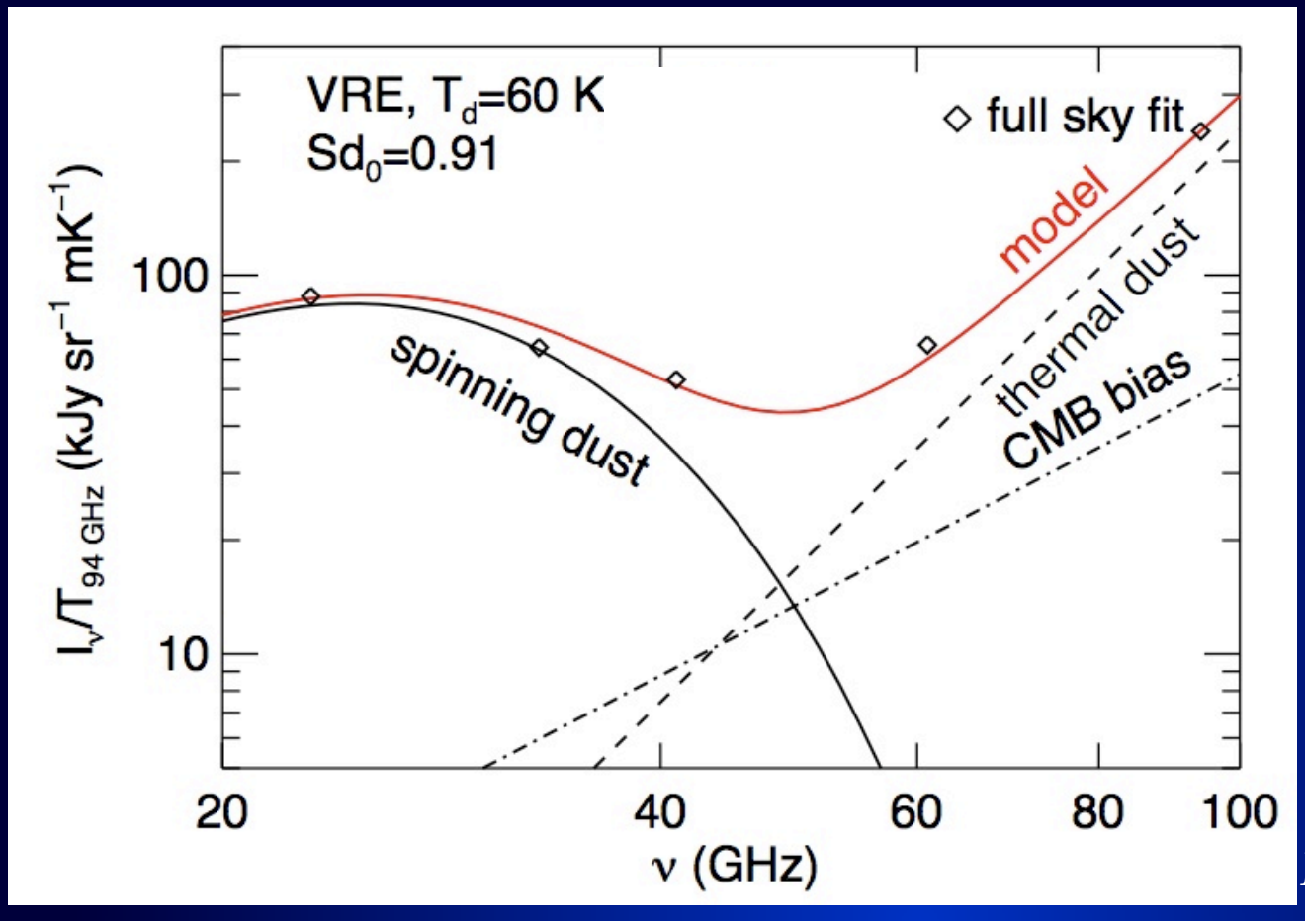

- T_0=0.8
- $Sd_0 \sim 0.9$
- β_0=0.95 D,
- $n_H \sim 10\ \mathrm{cm}^{-3}$

Hoang, Lazarian, & Draine 11

More regions with AME discovered by Planck

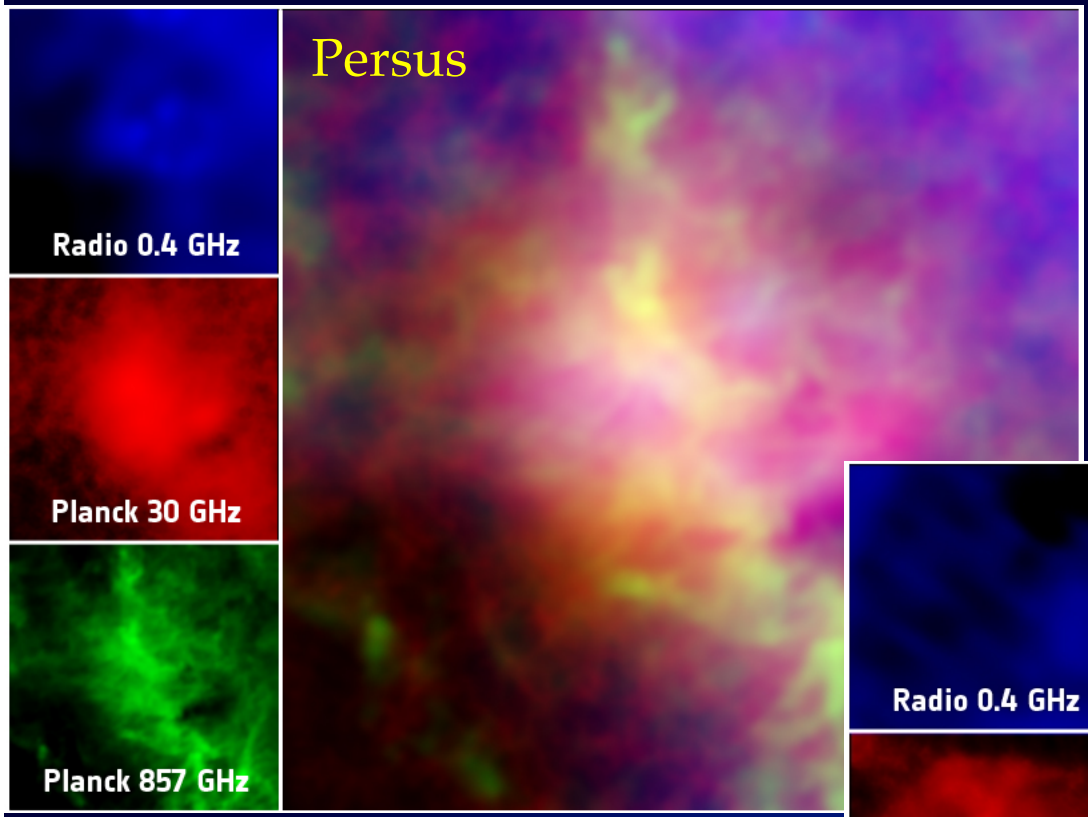

Credit: Planck

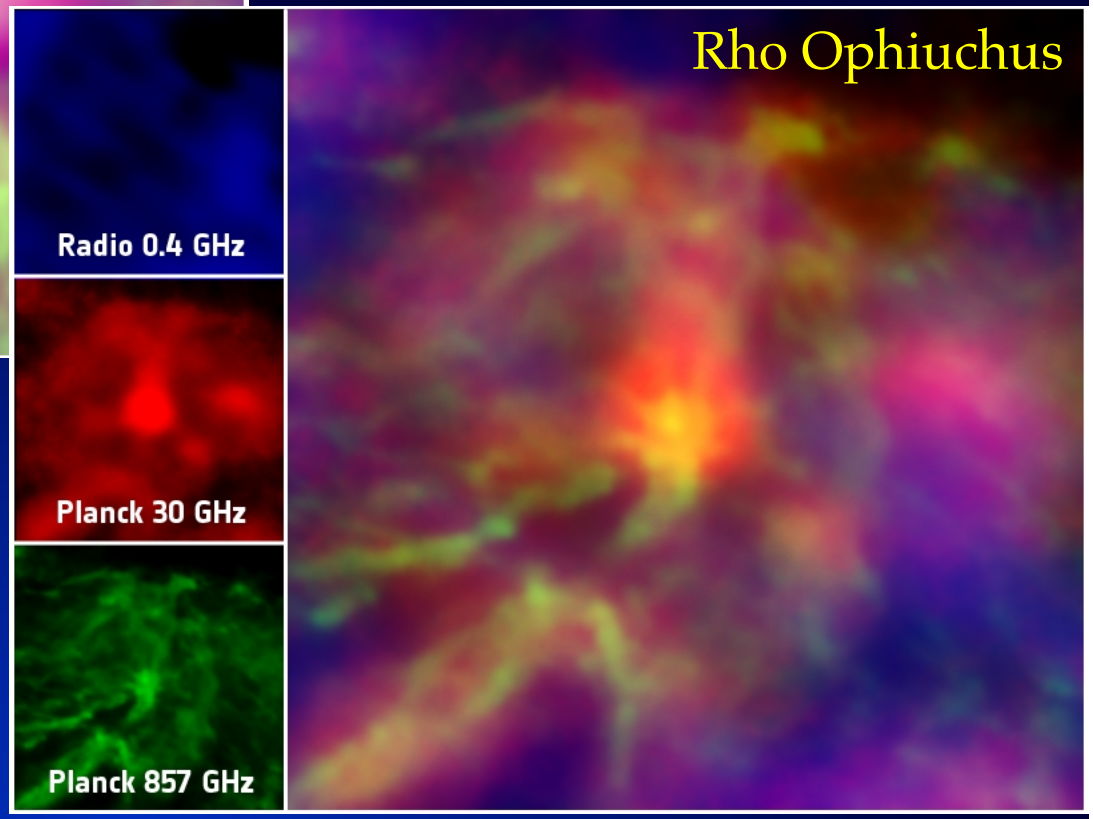

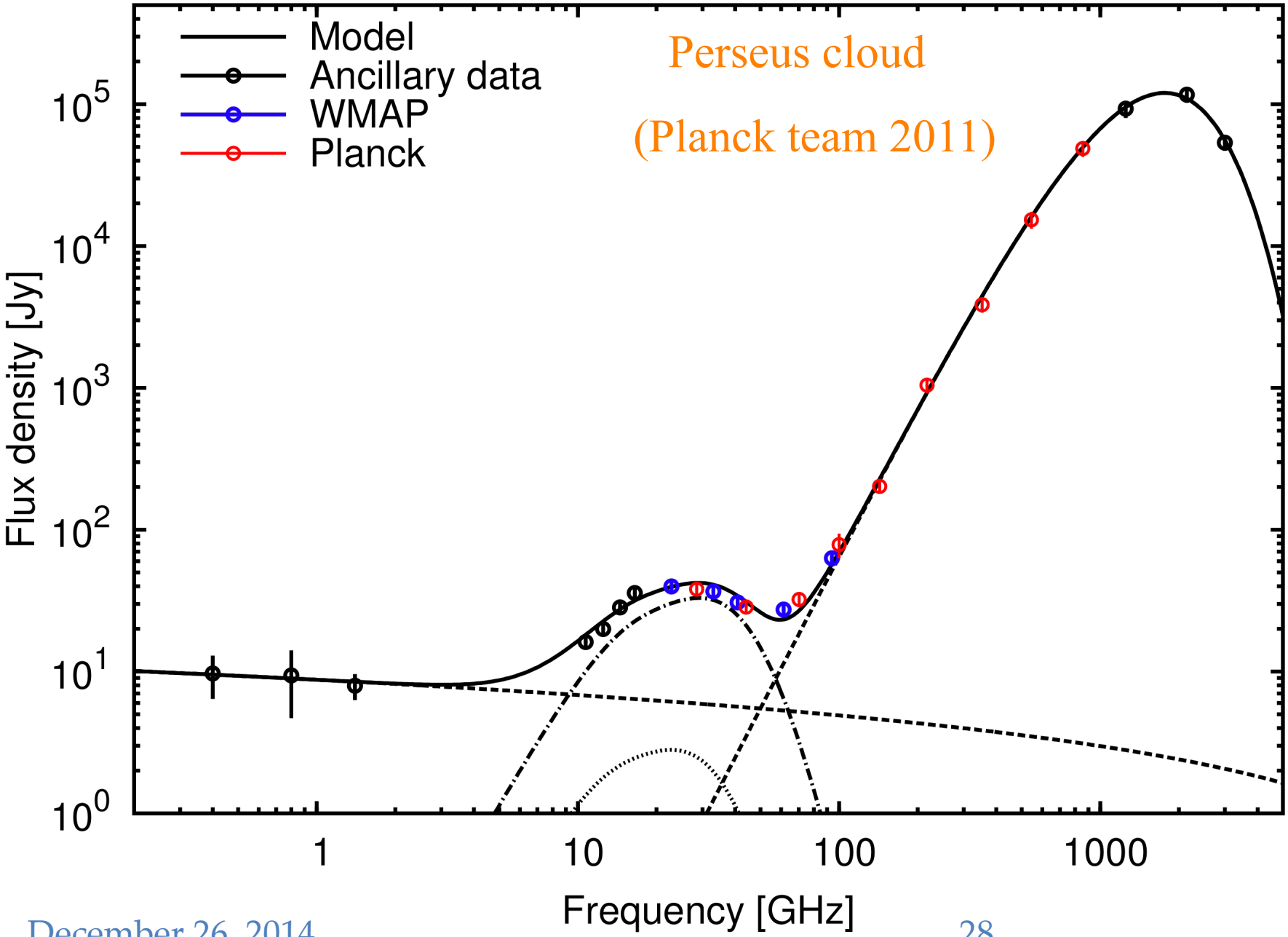
Model
Ancillary data
WMAP
Planck
Perseus cloud
(Planck team 2011)
Flux density [Jy]
Frequency [GHz]
10^0
10^1
10^2
10^3
10^4
10^5
1
10
100
1000

Magnetic dust: Emission from Magnetic Dipole Fluctuations

- Draine & Lazarian (1999) proposed magnetic dipole microwave emission as an alternative to spinning dust

- Draine & Hensley (2012, 2013) extended and improved the DL99, successfully explain submm excess

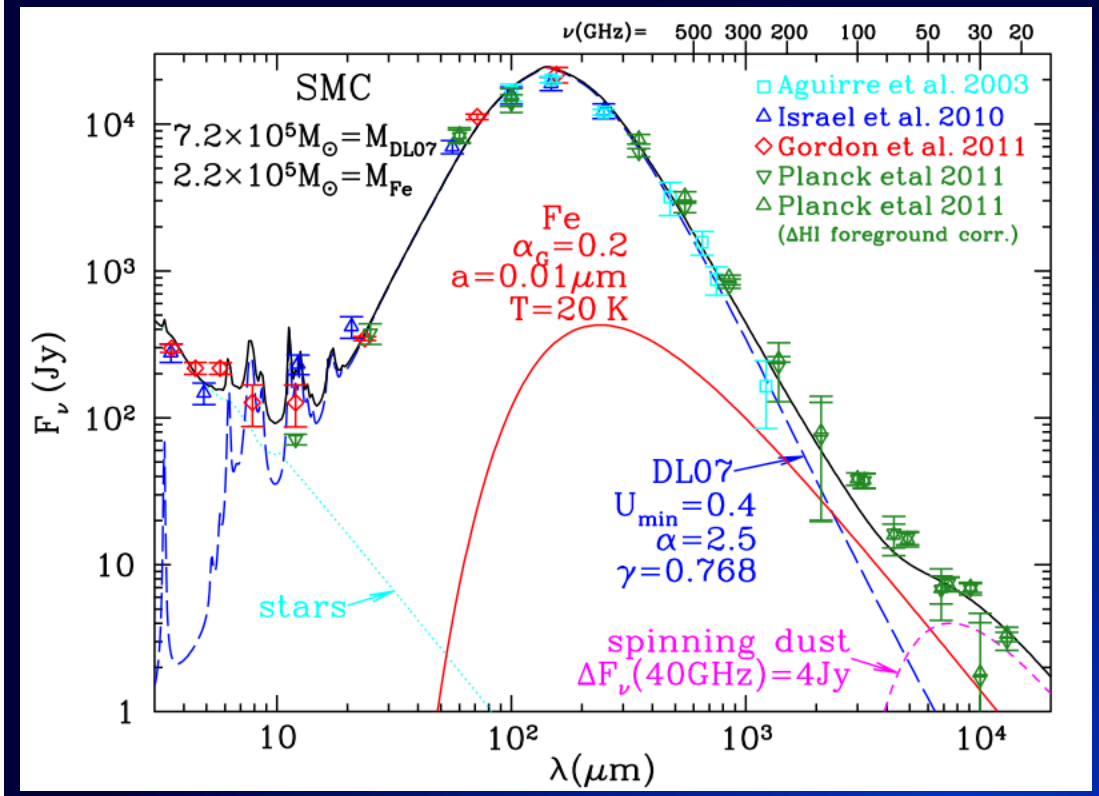

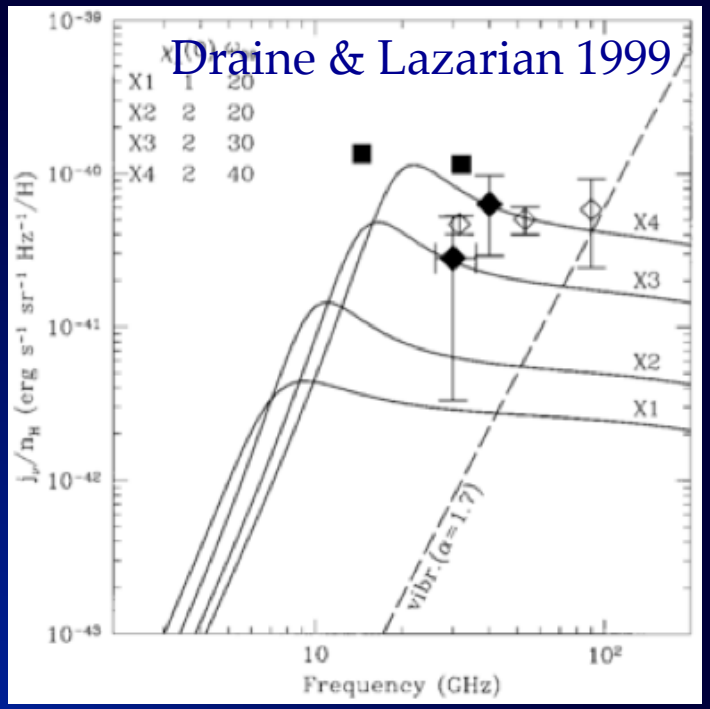

Draine & Hensley 2012

Polarization of Thermal Dust and Spinning Dust Emission

- What is dust polarization? Why do we care?
- Grain Alignment Theory
- Ab-initio Modeling of Polarization vs. Observations
- Inversion Technique and Self-consistent Modeling

1949: Discovery of Starlight Polarization

February 18, 1949, Vol. 109 SCIENCE 165

Polarization of Light From Distant Stars by Interstellar Medium

W. A. Hiltner

Yerkes Observatory, University of Chicago

IN THE COURSE OF PHOTOELECTRIC OBSERVATIONS made last summer with the 82-inch telescope of the McDonald Observatory (University of Texas) the writer found that the light from distant galactic stars is polarized. Polarizations as high as 12 percent were found. The plane of polarization appears to be close to the galactic plane in the cases examined. More recently control measures were made at the Lick Observatory, thanks to the courtesy of Director Shane and Dr. G. Kron; and during December the work at the McDonald Observatory was extended to different regions of the Milky Way.

In view of the unexpected nature of this result the circumstances leading to its discovery are recorded. Photometric observations for the detection of partially polarized radiation from eclipsing binary stars have been in progress at the Yerkes Observatory for several years with a view to establishing observationally the effect pointed out by Chandrasekhar that the continuous radiation of early-type stars should be polarized (*1, 2*). On the assumption that the opacity of early-type stars is due to scattering by electrons, the continuous radiation emerging from a star should be polarized with a maximum of polarization of 11 percent at the limb. Since the presence of this polarization can be detected only when the early-type star is partially eclipsed by a larger-type companion of the system, the effect is masked by radiation from this companion so that the expected maximum observable effect was only of the order of 1.2 percent in one case investigated (RY Persei).

At this stage Dr. John Hall, of Amherst College, proposed to the writer a program of collaboration whereby Dr. Hall would construct a "flicker" photometer which was to be tested jointly at the McDonald Observatory. Independently the writer was developing his own equipment which used polaroids. Dr. Hall's equipment was tested in August 1947, during a short session at the McDonald Observatory, but no dependable results were obtained and it was found that the equipment had to be remodeled. Unfortunately, Dr. Hall was unable to come for a second trial period, scheduled for August 1948.

Meanwhile the writer's own equipment was completed and put to use during the summer of 1948 and was found satisfactory. Certain Wolf Rayet stars which were known or suspected to be eclipsing binaries were examined for polarization. Fairly large polarizations were found, but *they did not appear to depend on the phase of the binary motion.* The possibility of instrumental polarization was considered, of course, but ruled out by control measures on check stars. The Wolf Rayet stars give the following results:

Star	*Polarization*	
	%	Position angle
CQ Cep	10.0	62°
BD 55°2721	8.0	44
WN Anon*	12.5	44

*Coordinates: $22^h08^m + 57°26'$ (1945); 12.5 magnitude.

The control stars had similar color and brightness, but showed no polarization except for one object, BD 55°2723, which gave 3 percent. This star, however, is a giant and more distant than the other control stars. Similar observations made on a group of Wolf Rayet stars in Cygnus showed no appreciable polarization, while two stars in Scutum gave positive results. Other regions, such as the double cluster in Perseus, also show polarization with values ranging up to 12 percent.

We conclude from the positive and negative results quoted that the measured polarization does not arise in the atmospheres of these stars but must have been introduced by the intervening interstellar medium. If this conclusion is accepted, a new factor in the study of interstellar clouds is introduced. Further observations are in progress for relating this phenomenon with other observable characteristics of interstellar medium. As has been stated, the results already at hand indicate that the plane of polarization approximates the plane of the galaxy.

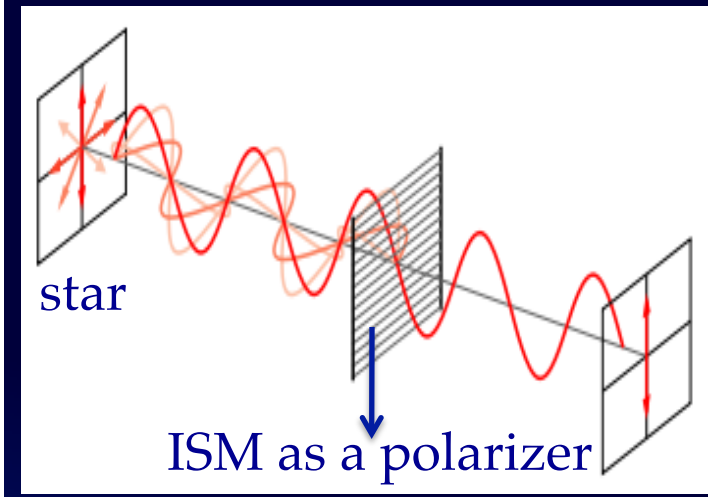

166 SCIENCE February 18, 1949, Vol. 109

Observations of the Polarized Light From Stars

John S. Hall

U. S. Naval Observatory, Washington, D. C.

PHOTOELECTRIC OBSERVATIONS of the polarization of starlight made during the period November 1948 to January 1949 with the 40-inch reflector at Washington substantiate the hypothesis of W. A. Hiltner (*2*) that this effect is produced by interstellar matter. Furthermore, the percentage of polarization appears to be independent of wavelength; and the plane of polarization (plane containing the magnetic vector and the line of sight) appears to have no one preferential orientation.

The observations were obtained with a photoelectric polarizing photometer (*1*) built at Amherst College in 1946 with the aid of a grant from the Research Corporation of New York. The light from a star is collimated and directed through a cover glass, which serves as a calibrating device, and then through a Glan-Thompson prism rotated at 15 cycles per second to a 1P21 photomultiplier. The 30-cycle voltage developed by the polarized component of the light

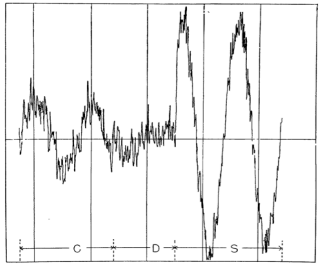

FIG. 1. Star HD 19820, a reddened star of spectral type O8. Polarization, 5.0%; position angle of the plane of polarization, +30°.

stars showing large and small percentages of polarized light are shown in Figs. 1 and 2. The vertical lines represent two-minute intervals. The trace during interval *S* is produced by polarized light from the star. During interval *D* a quartz depolarizer is placed in the light path, and *C* is the result when the cover glass is tilted 20° about an axis whose position angle is arbitrarily set at 94°. The starlight was already depolarized during the interval *C*. The plane of polarization is defined by the direction of the light and the axis about which the glass is tilted. A 20° tilt corresponds to 1.4% polarization.

The percentages of polarization of the light from 27 early-type stars are shown in Fig. 3 as a function of the color excesses determined by Stebbins and Huffer (*3*). A strong correlation is obvious; the scatter, however, is much greater than the accidental errors of the observations.

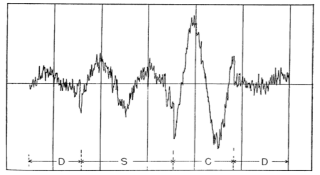

FIG. 2. Star HD 24760, ε Persei. This bright star is not generally considered to be a reddened B-type star. Polarization, 0.5%; position angle, −68°.

The dependence of polarization on color was determined on three nights from observations of ζ Persei using Schott filters UG1 and BG14 for the ultraviolet region and RG1 or a Wratten yellow filter for the red region. The effective wavelengths of the two spectral regions were near 3,700 A and 6,200 A. The observed percentages with the ultraviolet filter were 2.0, 1.6, and 1.8; and with the red filter 1.6, 1.0, and 2.2. The

Polarization Spectrum of Starlight

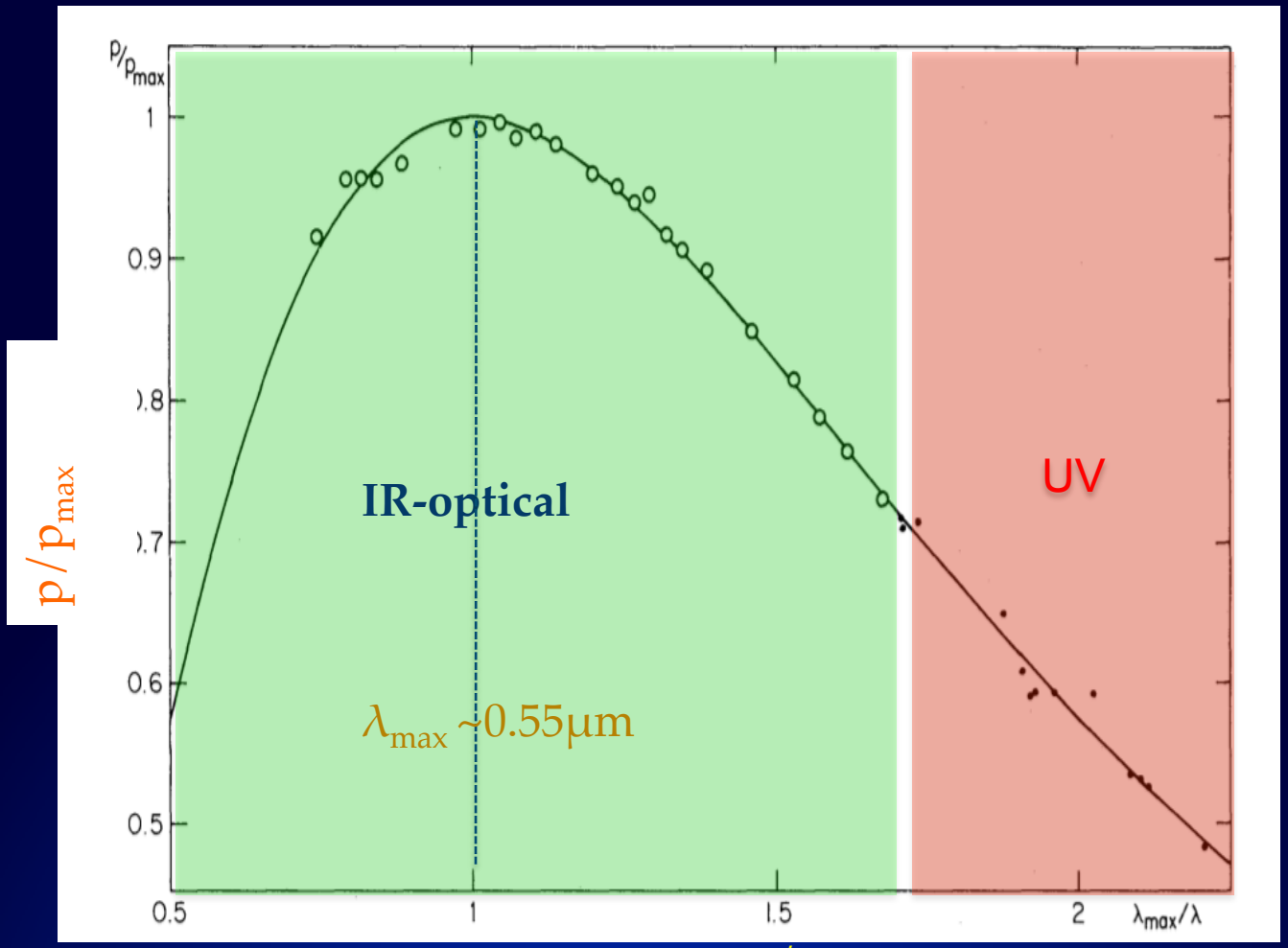

$$p(\lambda) = p_{\max} \exp\left[-K \ln^2\left(\frac{\lambda_{\max}}{\lambda}\right)\right]$$

K =1.15, Serkowski et al. 1973, 1975

$K = 1.66\lambda_{max} + 0.01$ (Whittet + 92)

Gravitational Waves via B-mode Polarization

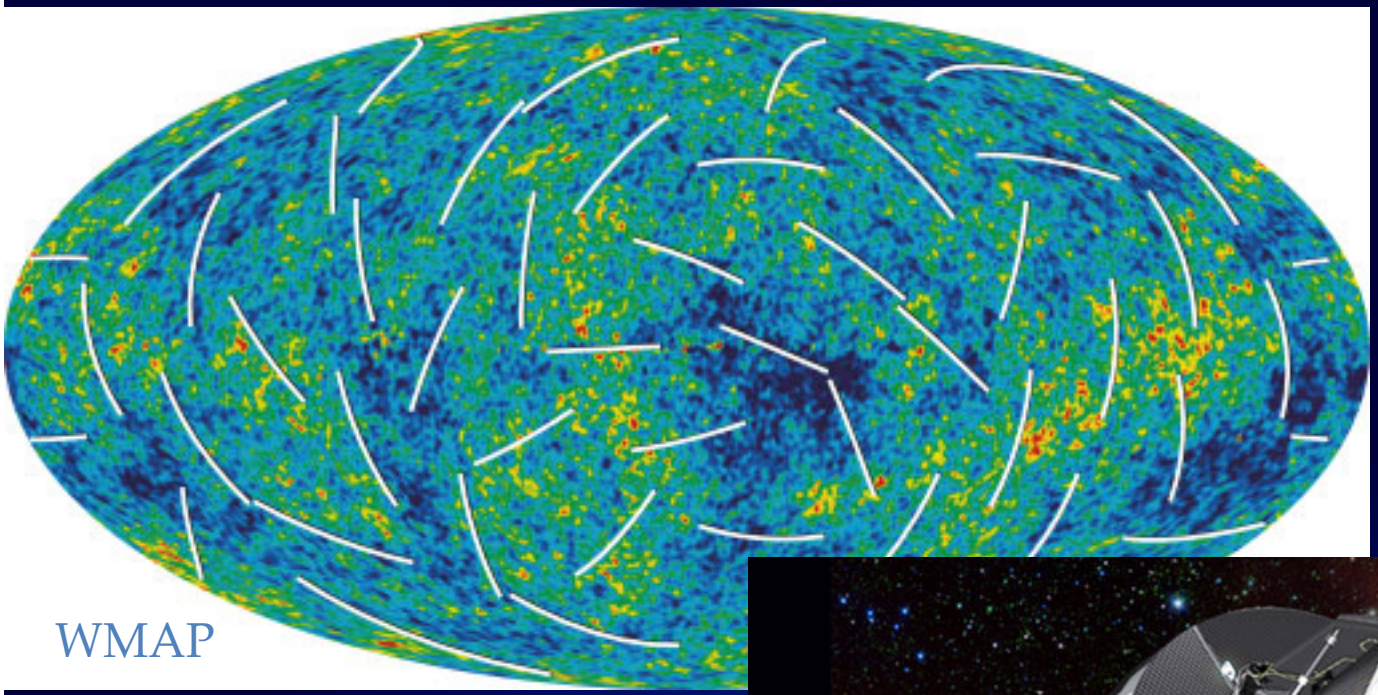

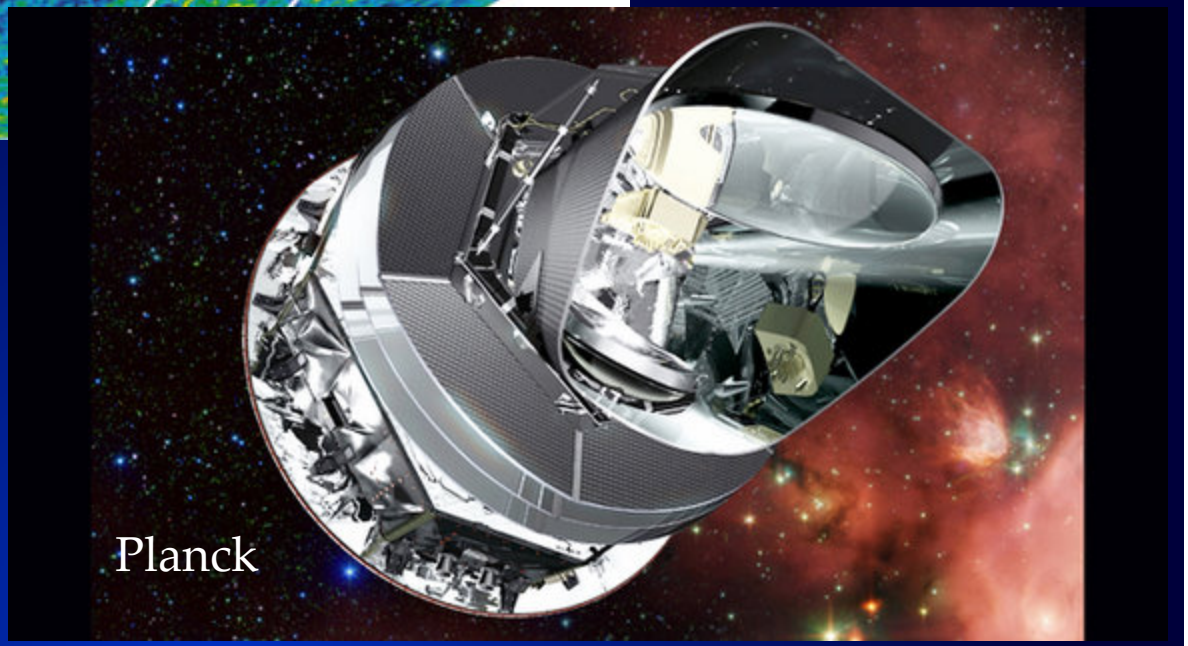

Separating Polarized CMB Components

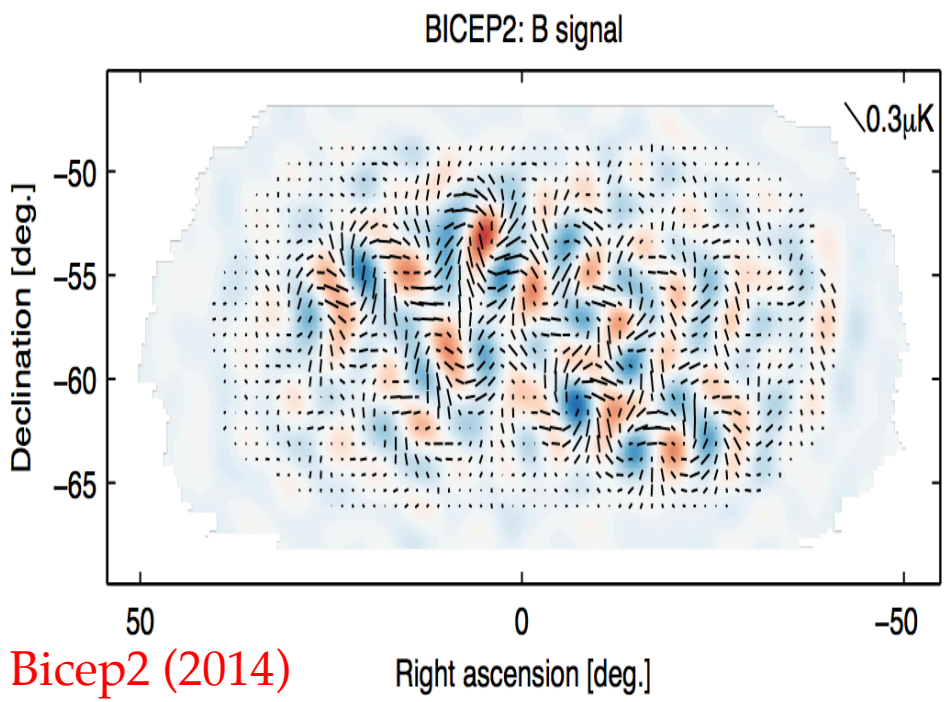

Bicep2 (2014)

The simplest and most economical remaining interpretation of the B-mode signal which we have detected is that it is due to tensor modes — the IGW template is an excellent fit to the observed excess. We therefore proceed to set a constraint on the tensor-to-scalar ratio and find $r = 0.20^{+0.07}_{-0.05}$ with $r = 0$ ruled out at a significance of 7.0σ. Multiple lines of evidence have been presented that foregrounds are a subdominant contribution: i) direct projection of the best available foreground models, ii) lack of strong cross correlation of those models against the observed sky pattern (Figure 6), iii) the frequency spectral index of the signal as constrained using BICEP1 data at 100 GHz (Figure 8), and iv) the spatial and power spectral form of the signal (Figures 3 and 10).

Subtracting the various dust models and re-deriving the r constraint still results in high significance of detection. For the model which is perhaps the most likely to be close to reality (DDM2 cross) the maximum likelihood value shifts to $r = 0.16^{+0.06}_{-0.05}$ with $r = 0$ disfavored at 5.9σ. These high values of r are in apparent tension with previous indirect limits based on temperature measurements and we have discussed some possible resolutions including modifications of the initial scalar perturbation spectrum such as running. However we emphasize that we do not claim to know what the resolution is.

Planck intermediate results. XXX. The angular power spectrum of polarized dust emission at intermediate and high Galactic latitudes

ABSTRACT

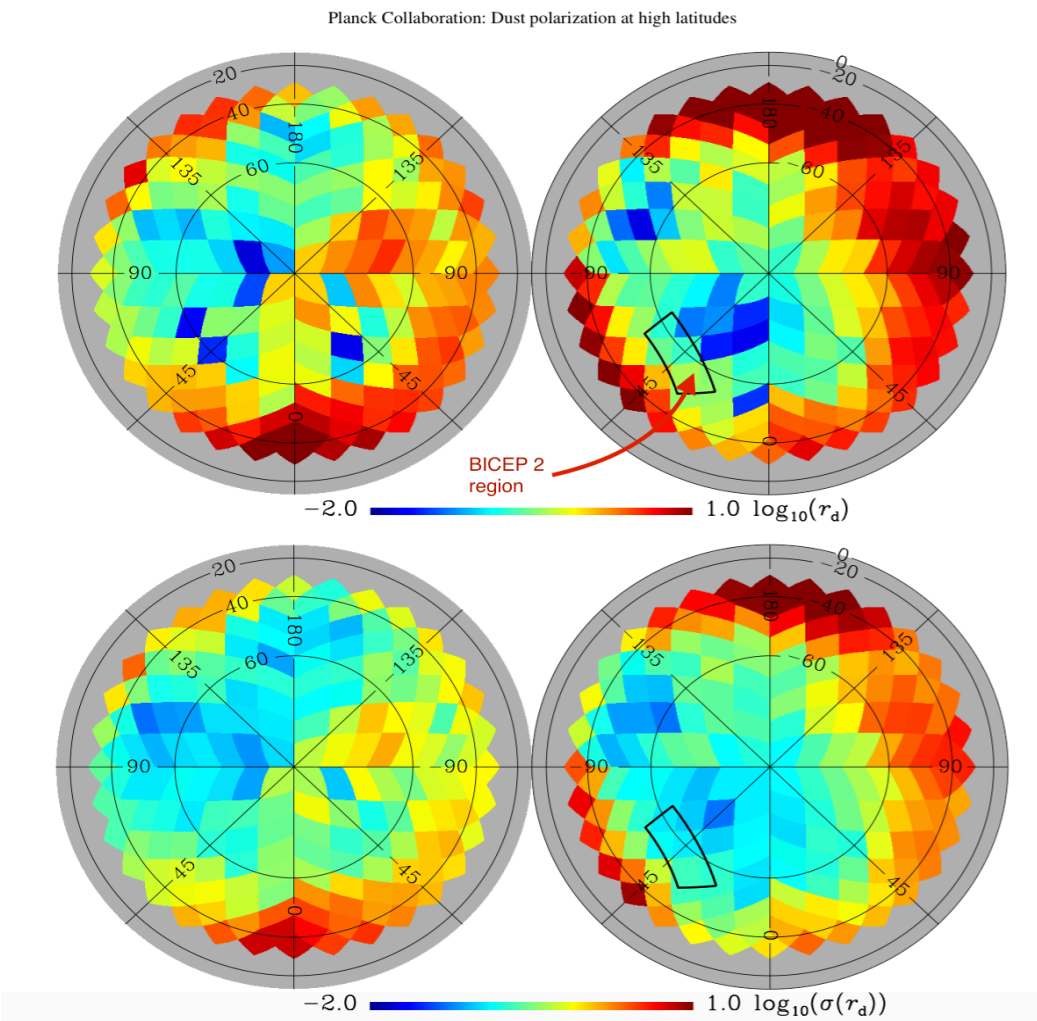

ound present in measurements of the polarization of the cosmic
xploit the uniqueness of the *Planck* HFI polarization data from 100
ver the multipole range $40 < \ell < 600$ well away from the Galactic
and allow a precise determination of the level of contamination for
e of Galactic dust, we show that general statistical properties of the
gular power spectra. The polarization power spectra of the dust are
2.42 ± 0.02. The amplitudes of the polarization power spectra vary
requency dependence of the dust polarization spectra is consistent
e lowest *Planck* HFI frequencies. We find a systematic difference
e verify that these general properties are preserved towards high
test dust-emitting regions there are no "clean" windows in the sky
out subtraction of foreground emission. Finally, we investigate the
xperiment. Extrapolation of the *Planck* 353 GHz data to 150 GHz
ipole range of the primordial recombination bump ($40 < \ell < 120$);
ertainty $(+0.28, -0.24) \times 10^{-2}\ \mu K^2_{CMB}$ from the extrapolation. This
ghlights the need for assessment of the polarized dust signal even
be reduced through an ongoing, joint analysis of the *Planck* and

Dust polarization used to test star formation theory

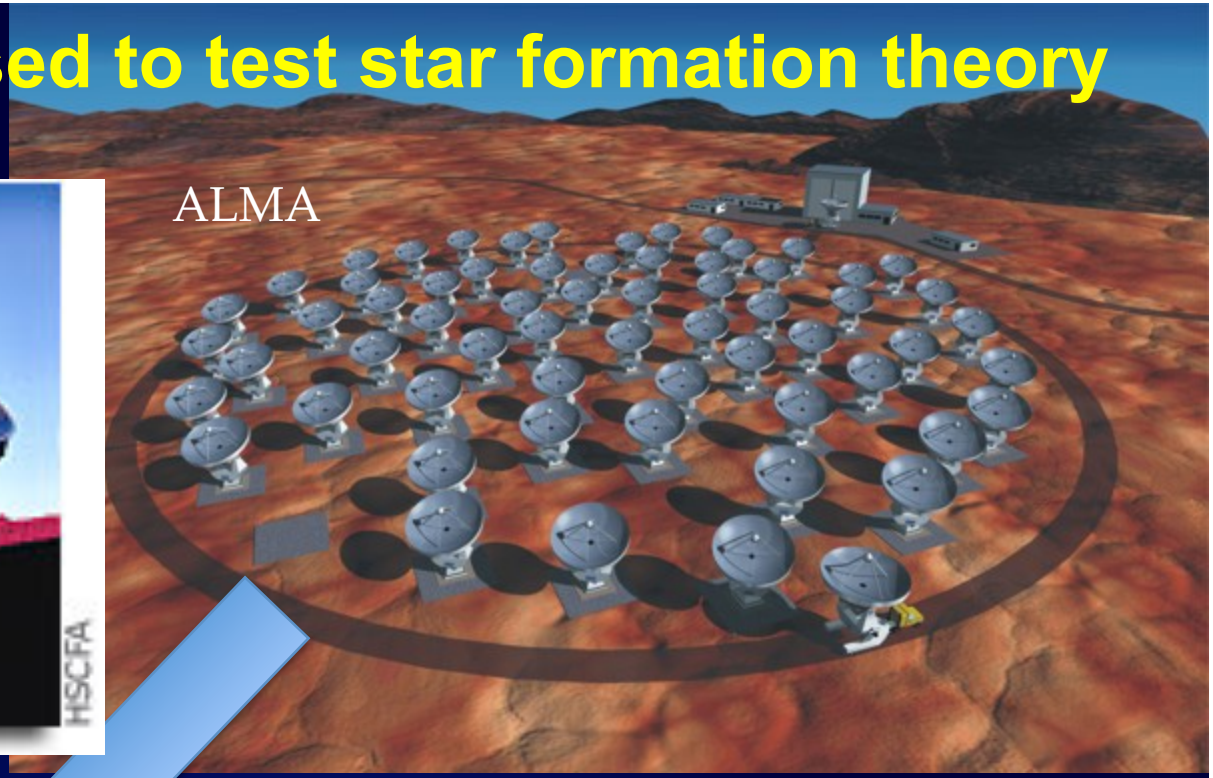

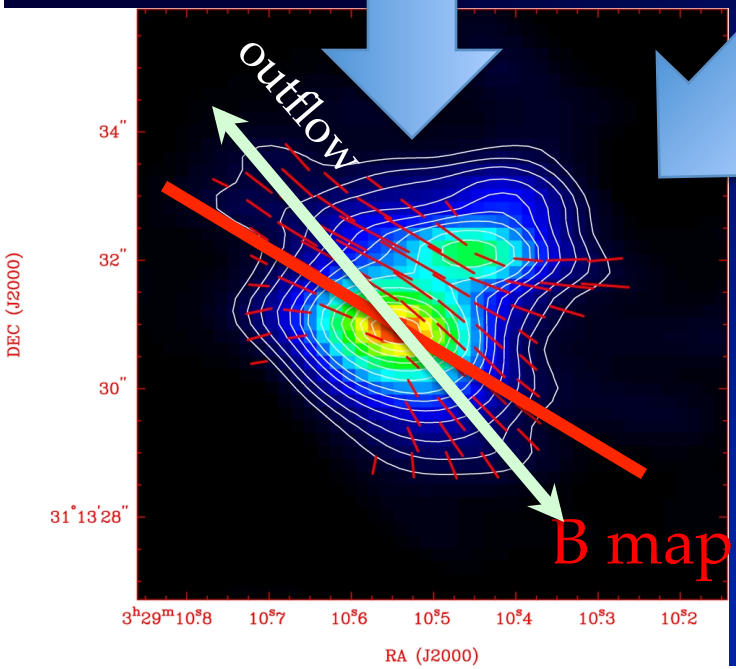

- Chandrasekhar-Fermi technique:

$$\frac{B_{\mathrm{POS}}}{\sqrt{4\pi\rho}} \propto \frac{\delta V}{\delta \phi}$$

- Mass to Flux ratio:

$$E_{gra}/E_{mag} = M/\Phi \sim N(HI)/B$$

- M/Φ and B-field and outflow allow us to test star formation theory

Not only to interpret observations but we must have predictive model, as well as quantitative predictions for CMB component separation. Therefore, a combination of various approaches is needed.

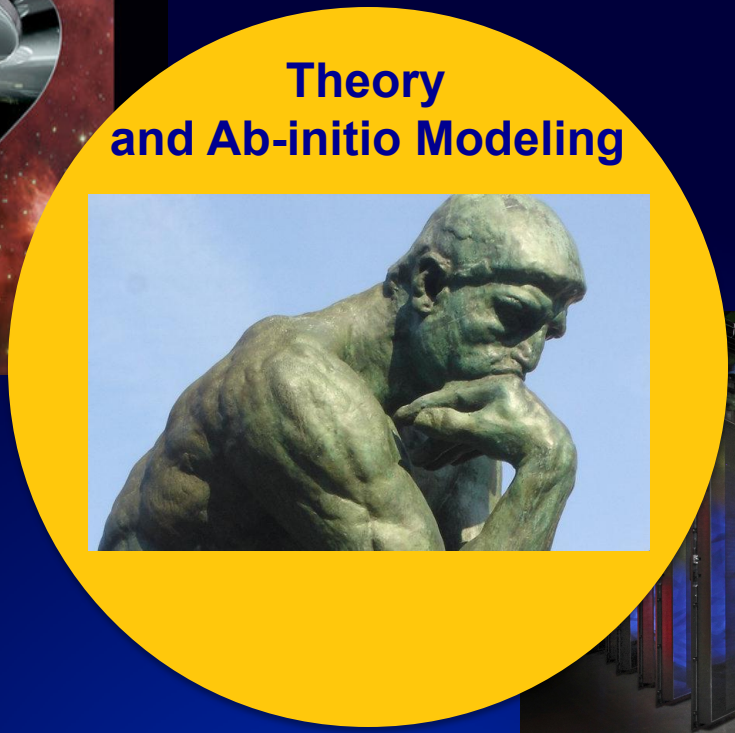

Dust grains must be aligned to produce starlight polarization.

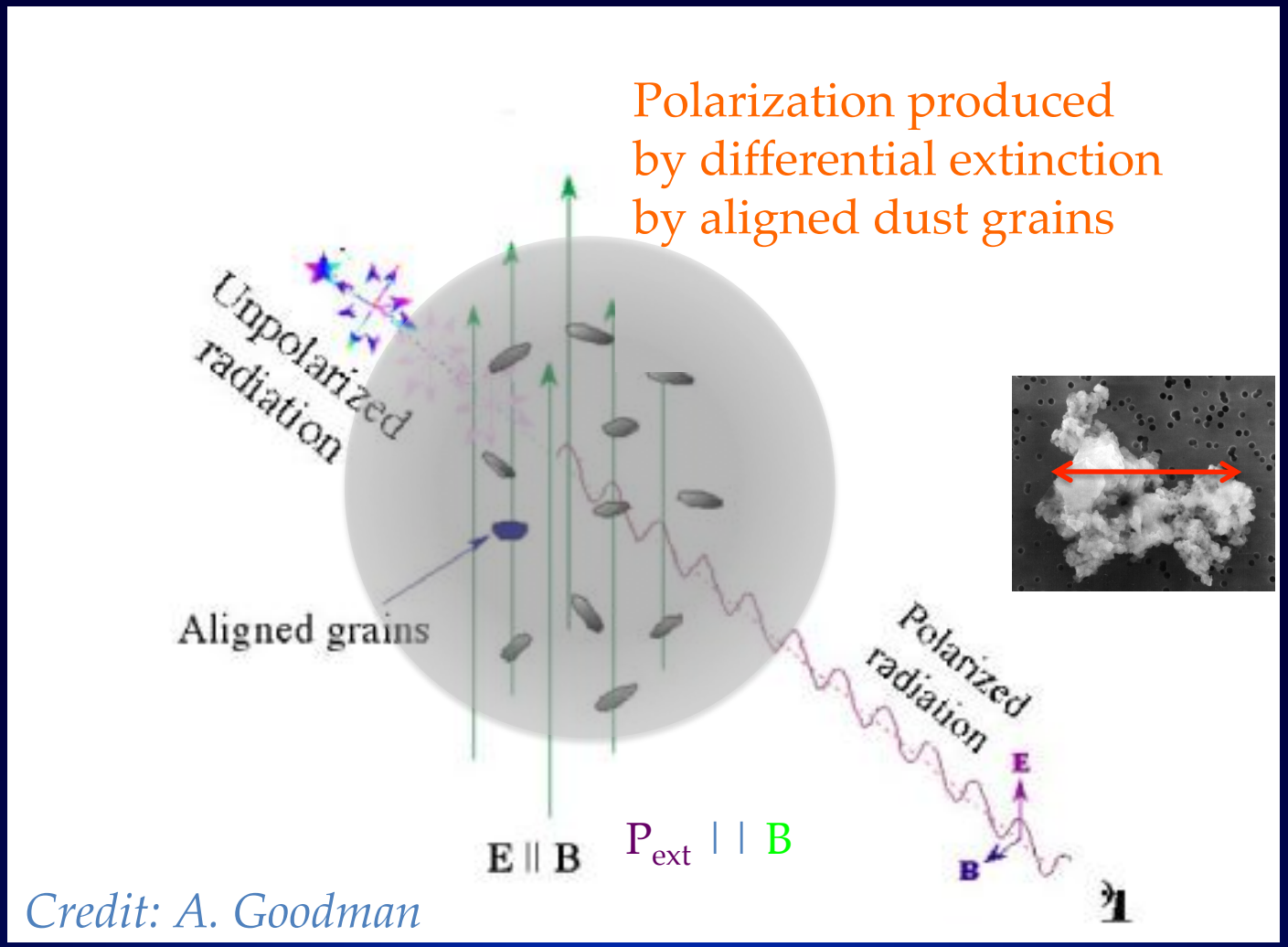

Credit: A. Goodman

Small grains (PAH) *weakly* aligned by paramagnetic relaxation

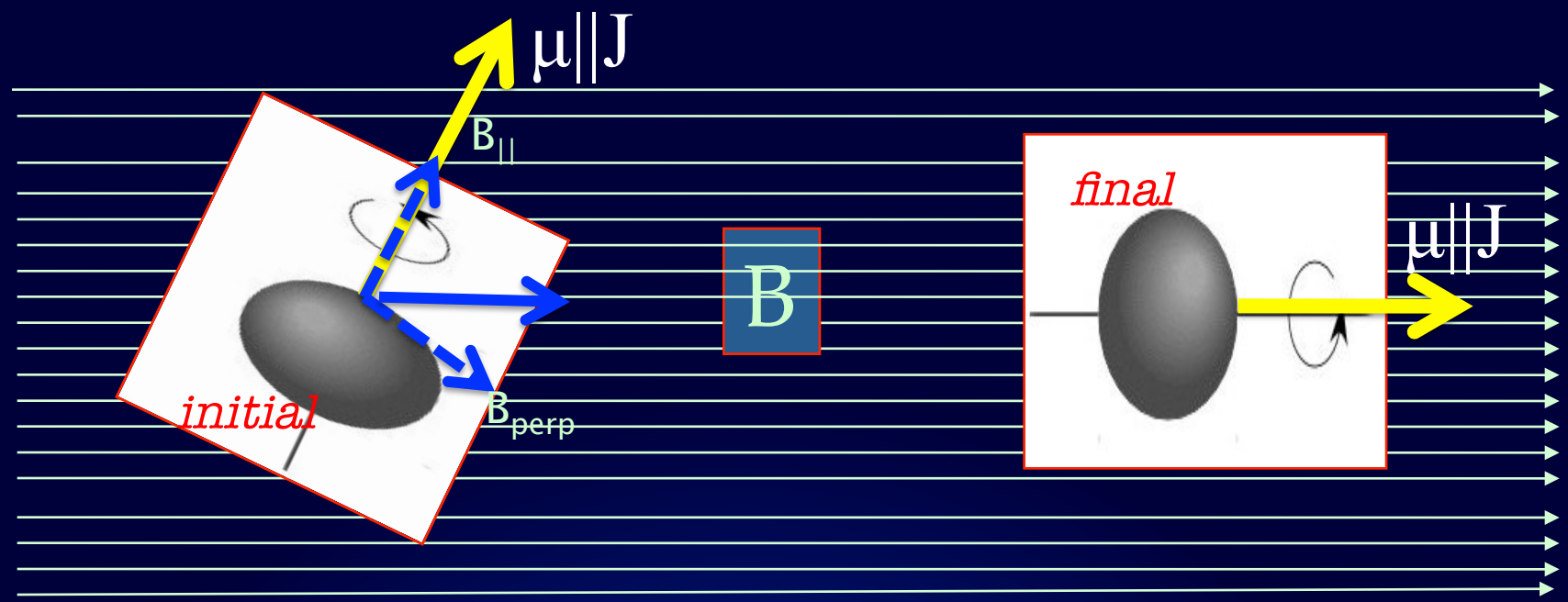

• Rotating magnetization by B_{perp} induces energy dissipation, decreasing the angle between J and B.

ISM

$$\tau_{DG} \approx 1.2\times10^{6}\left(\frac{B}{5\mu G}\right)^{-2}\left(\frac{a}{0.1\mu m}\right)^{2}\left(\frac{K(\omega)}{1.2\times10^{-13}\,s}\right)^{-1} yr$$

$$\tau_{drag} \approx 6.3\times10^{4}\left(\frac{a}{0.1\mu m}\right)\left(\frac{1}{1+F_{IR}}\right) yr$$

$$\frac{\tau_{DG}}{\tau_{drag}} \approx 20\left(\frac{a}{0.1\mu m}\right)\left(1+F_{IR}\right)$$

$\tau_{DG} < \tau_{drag}$ for $a \ll 0.1$ μm grains.

• Small grains can be aligned, big grains not

Theoretical calculations of paramagnetic alignment

- Evolution of angular momentum **J** in the lab frame:

$$dJ_i = A_i dt + \sqrt{B_{ii}}\, dq_i,\ i = 1-3$$

$$A_i = \sum_k \left\langle \frac{\Delta J_i^k}{\Delta t} \right\rangle, B_{ii} = \sum_k \left\langle \frac{(\Delta J_i^k)^2}{\Delta t} \right\rangle, \left\langle dq^2 \right\rangle = dt$$

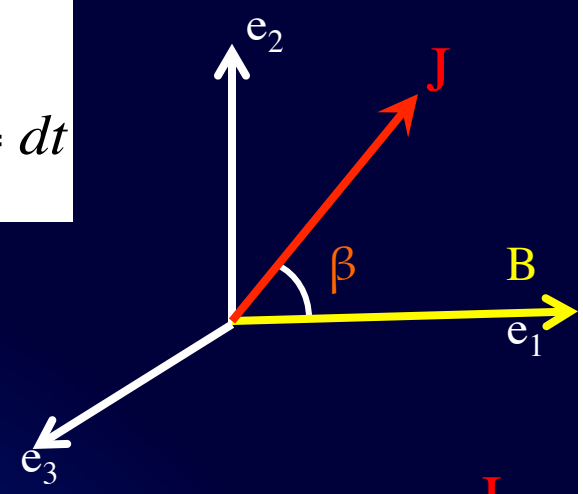

- Damping and excitation coefficients (A_i and B_{ii}) for:
  - dust-neutral and dust-ion collisions
  - infrared emission
  - plasma drag
  - paramagnetic relaxation, i.e., $\tau_{DG}(B)$
- Degrees of alignment:

  $R = \langle G_X{}^* G_J \rangle$, $Q_J(J,B) = \langle G_J \rangle$, $Q_X(a_1,J) = \langle G_X \rangle$

  with $G_J = [3\cos^2\beta - 1]/2$, $G_X = [3\cos^2\theta - 1]/2$

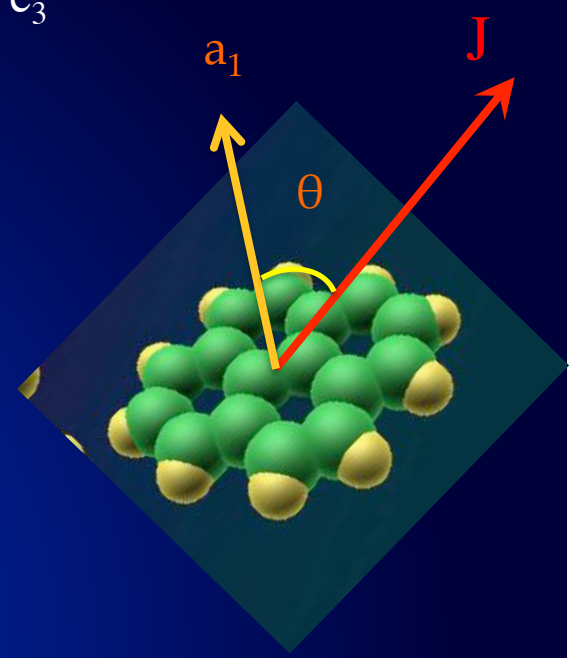

Paramagnetic alignment increases with magnetic strength.

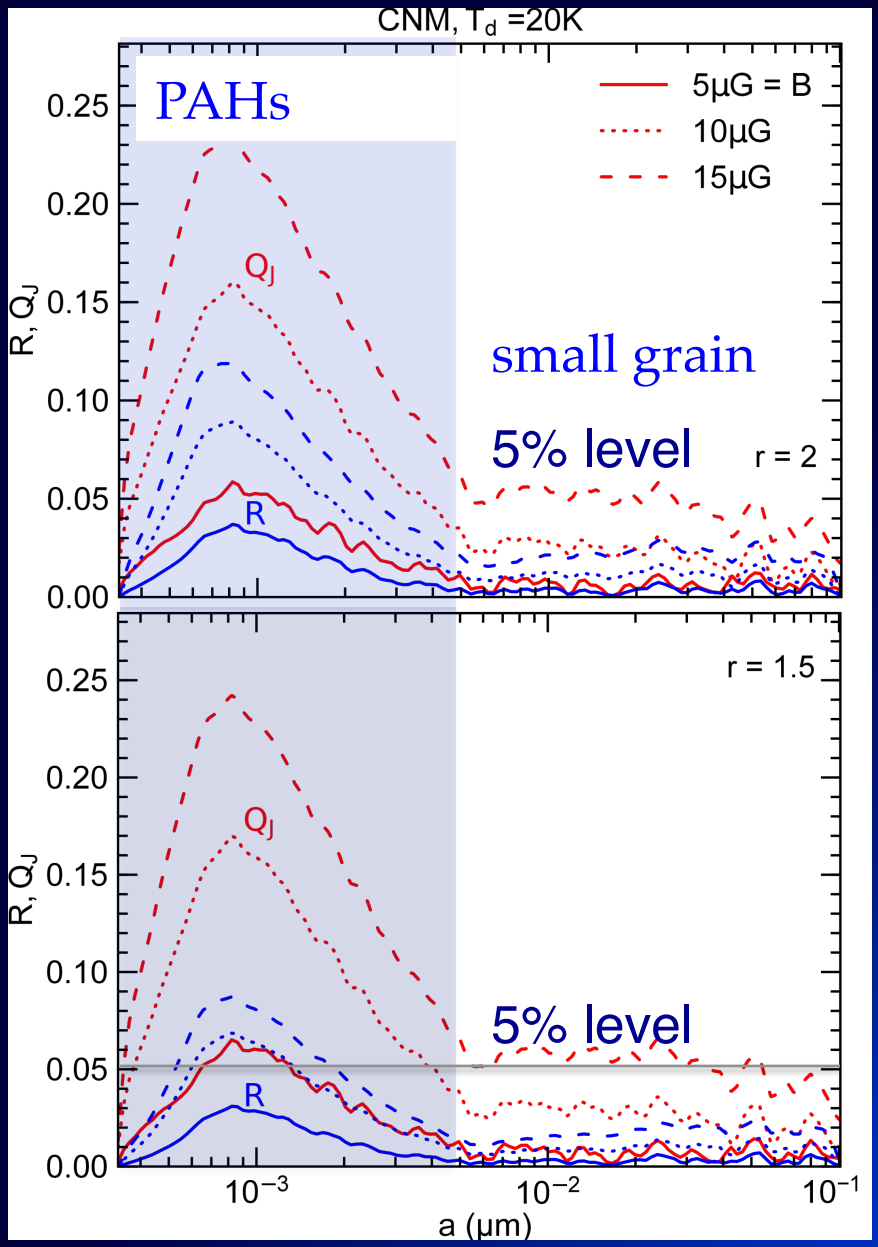

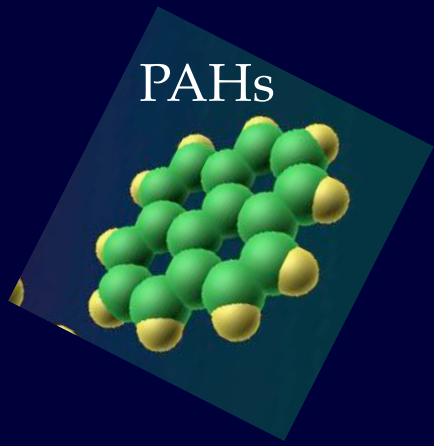

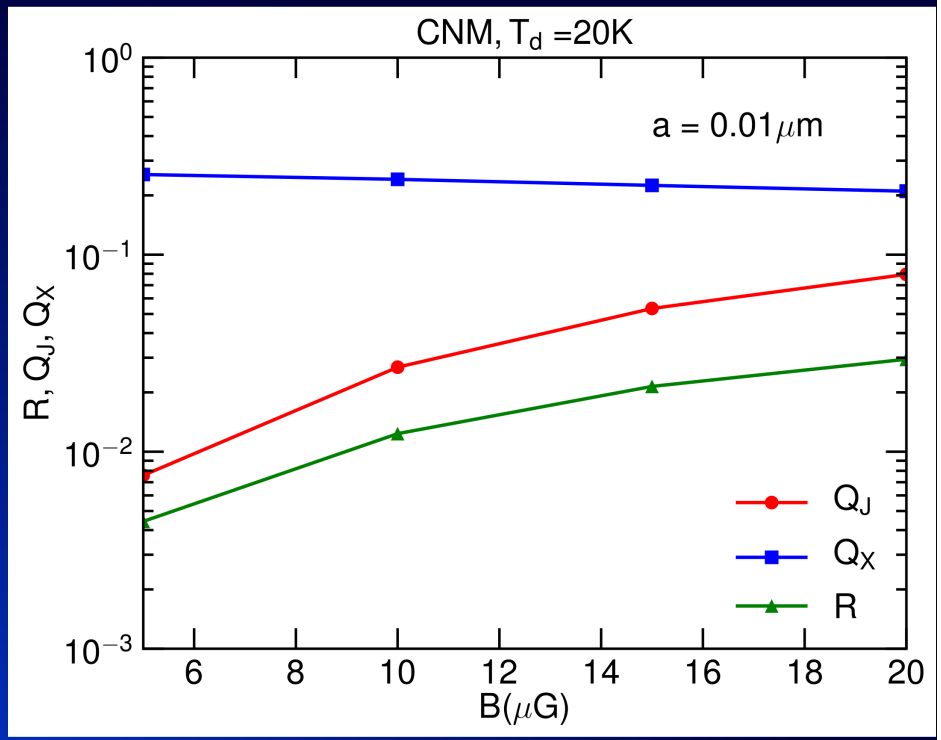

Hoang et al. 2014b

Big grains are aligned by radiative torques acting on helical grains.

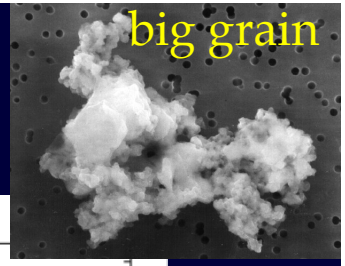

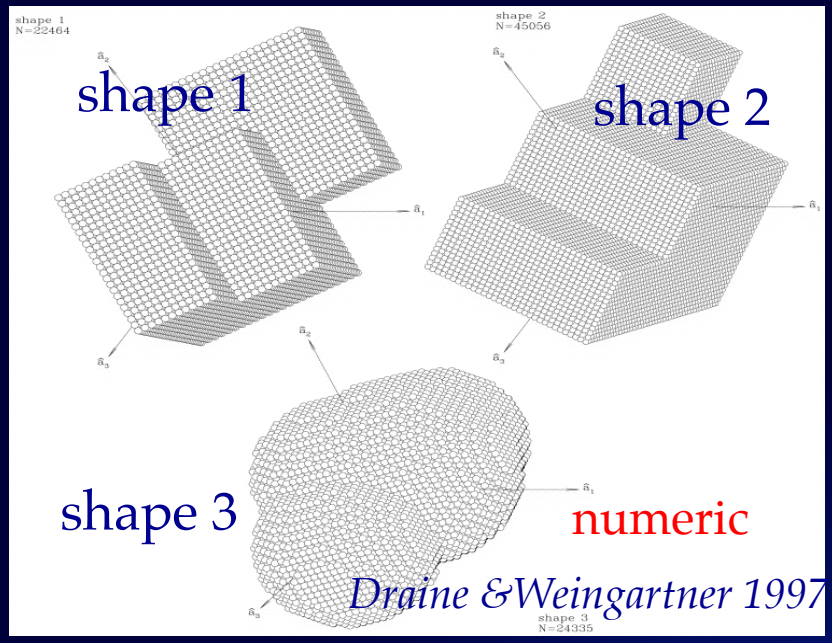

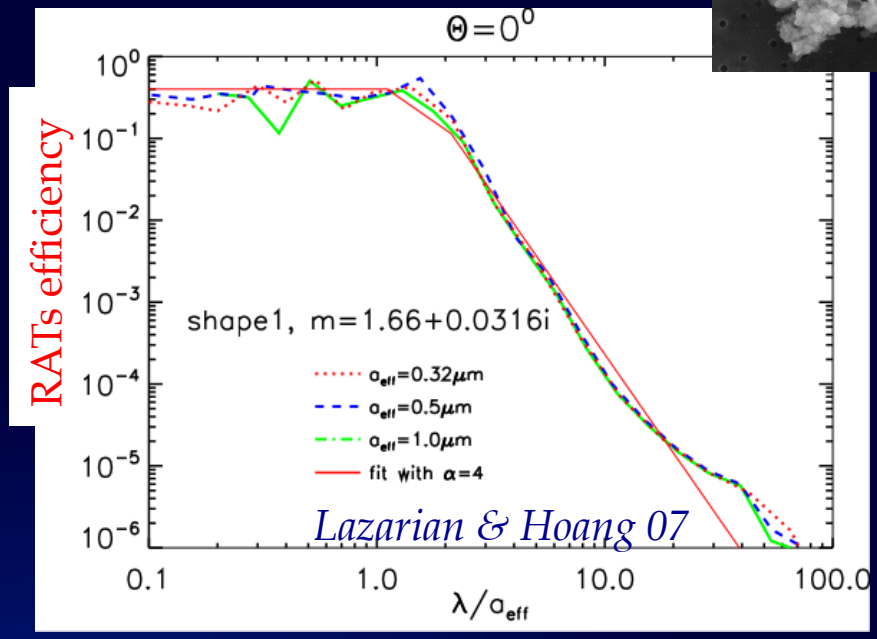

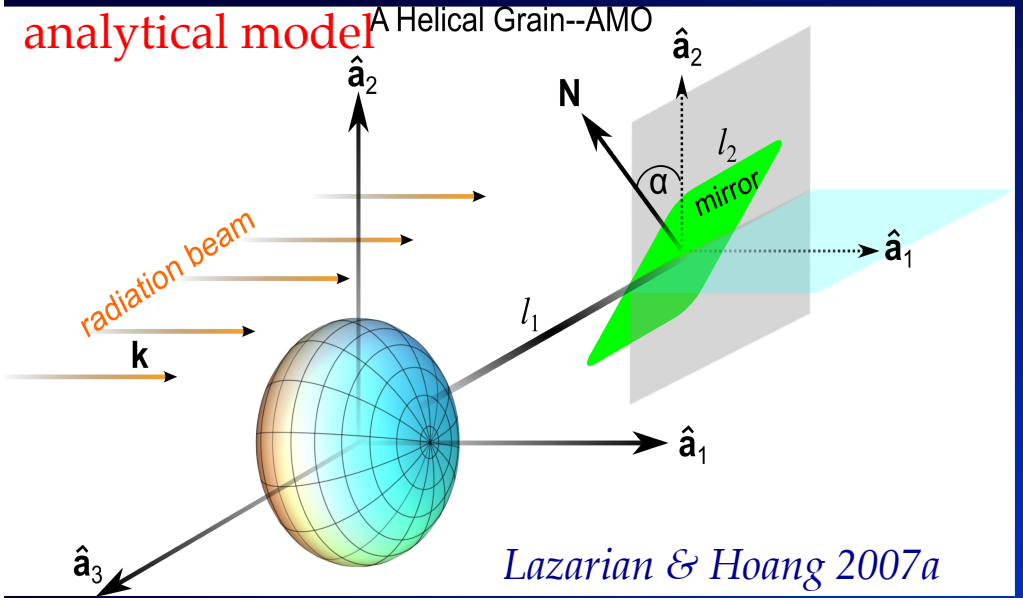

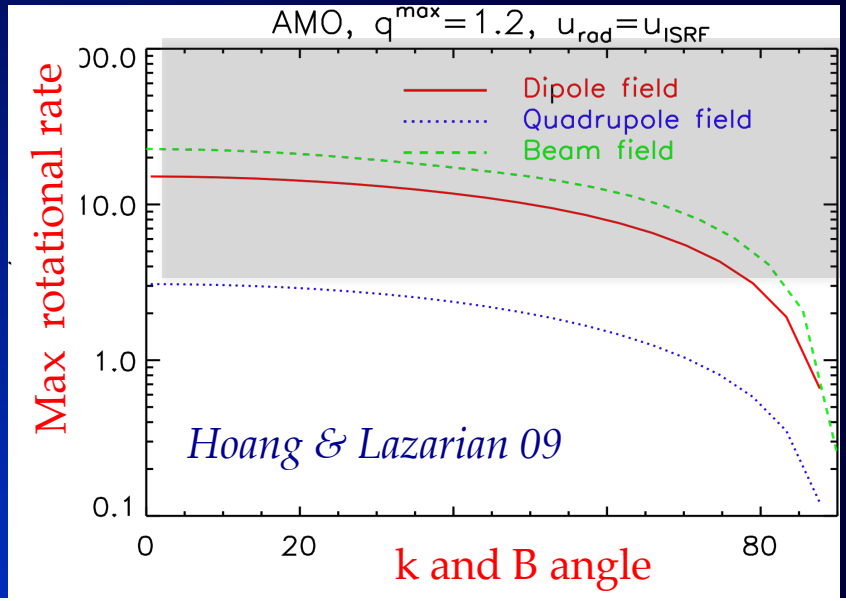

Basic Properties of RAT Alignment:
Grains are aligned with low-J and high-J attractors.

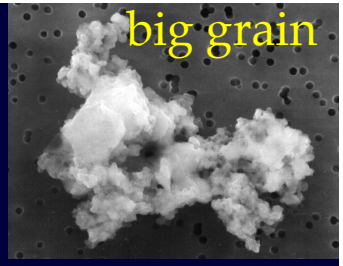

DDSCAT

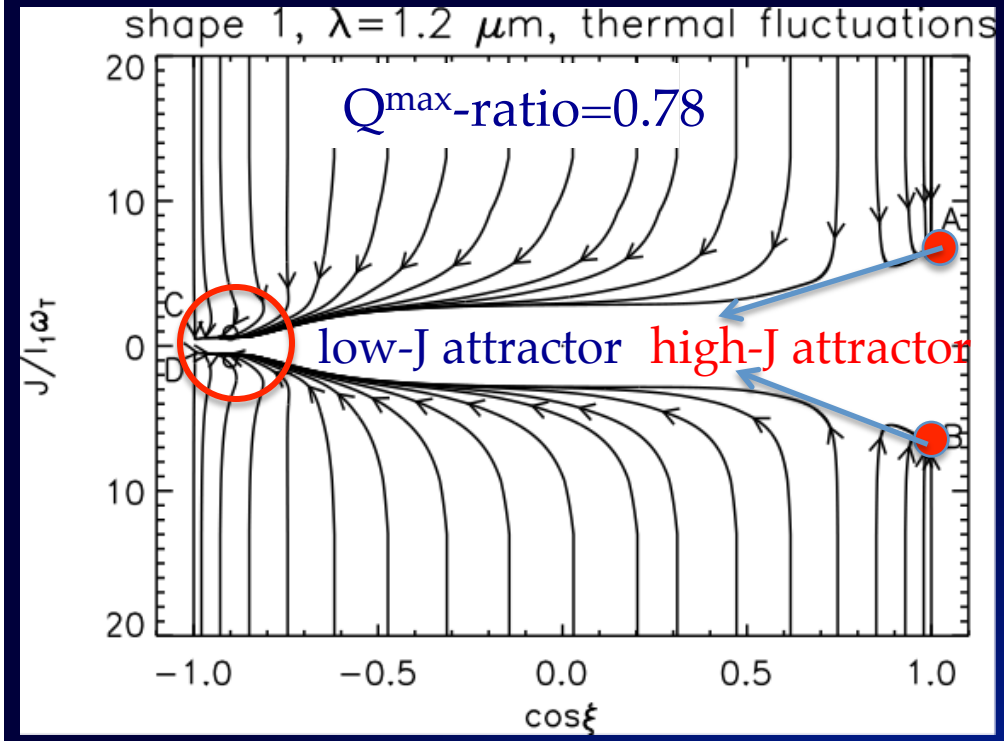

AMO

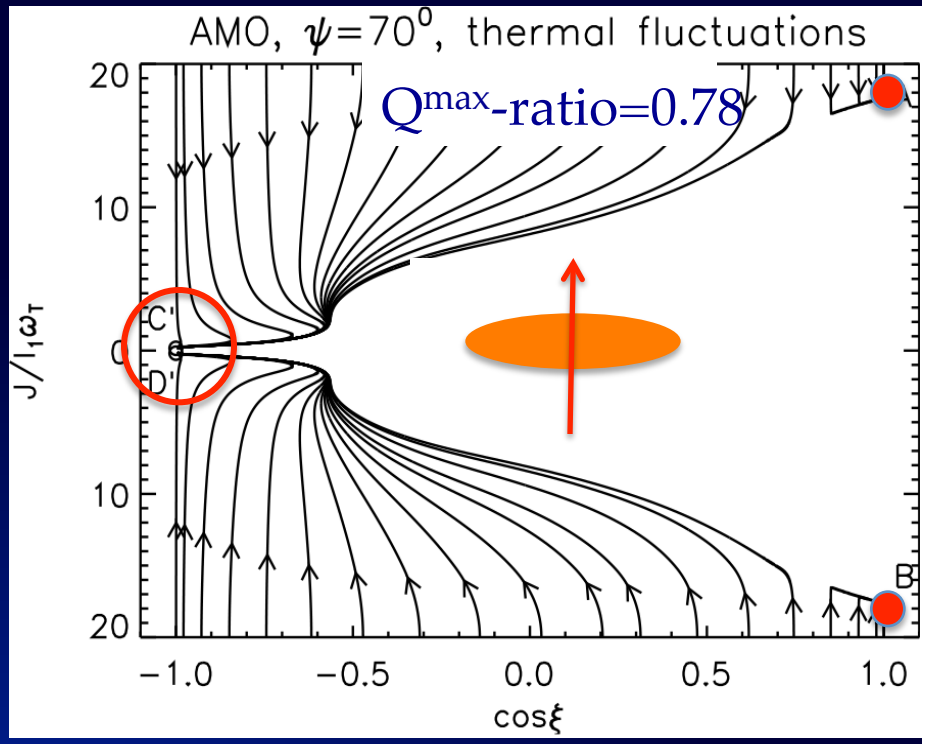

- Grains at high-J attractors are perfectly aligned, those at low-J attractors are partially aligned.

- AMO predicts the "right" alignment with long axes perpendicular to B.

Hoang & Lazarian 08

"Ab Initio" Modeling of Dust Polarization

grain size, shape, n_{gas}, T_{gas}, radiation field (intensity, k and B angle), and Q^{max}-ratio

Theory

Polarization

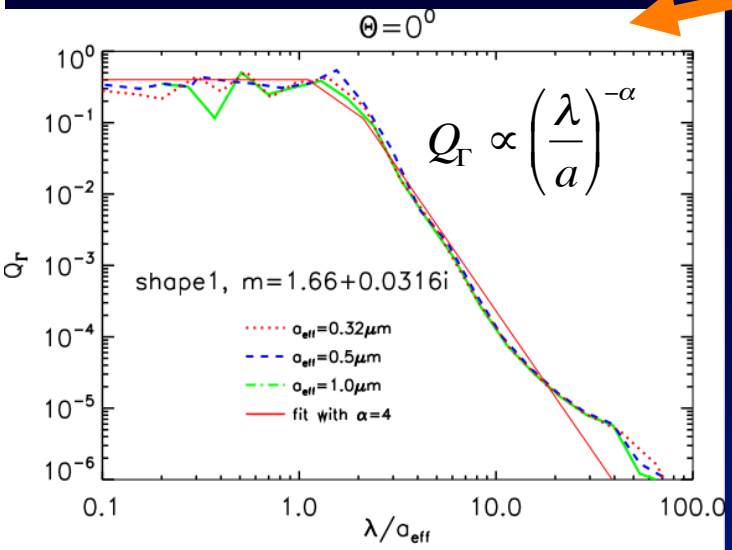

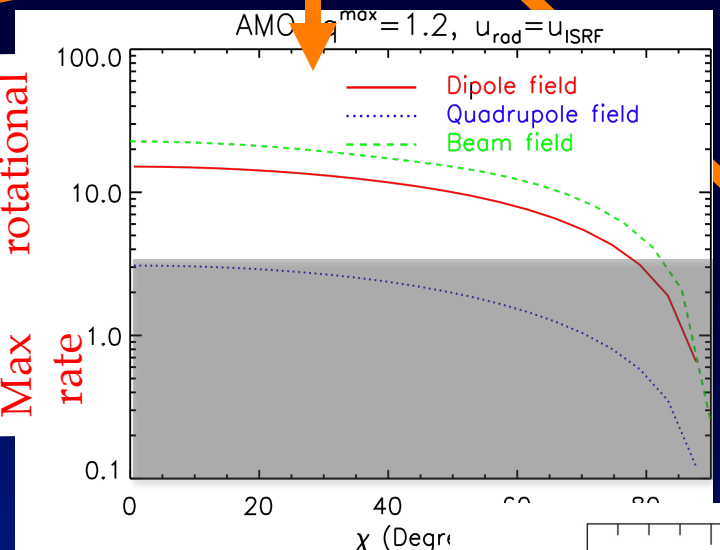

k and B angle

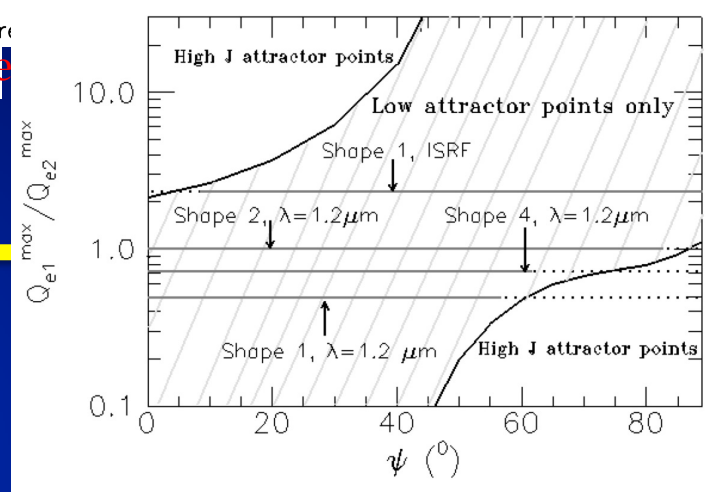

- Critical size of aligned grains: a_{ali}
- Degree of grain alignment: R

$$\frac{\sigma_{pol}}{N_H} = \int_{a_{ali}}^{a_{max}} da \frac{(C_\perp - C_\parallel)}{2} n_d(a) R(a) \cos^2\gamma$$

Polarization from Starless Cloud

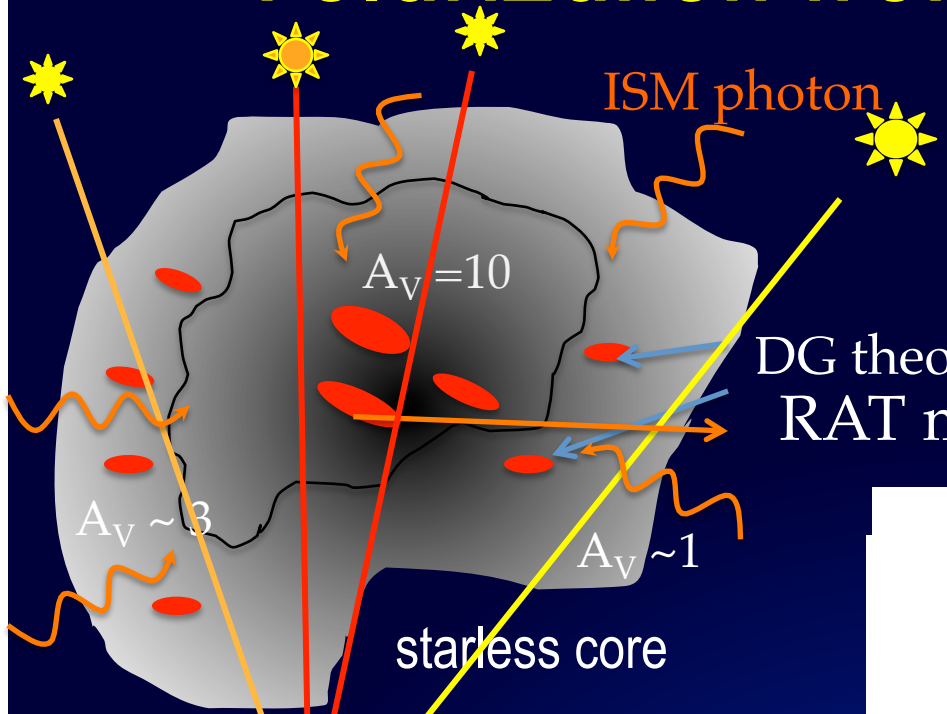

DG theory: grains aligned in interface, not core
RAT model

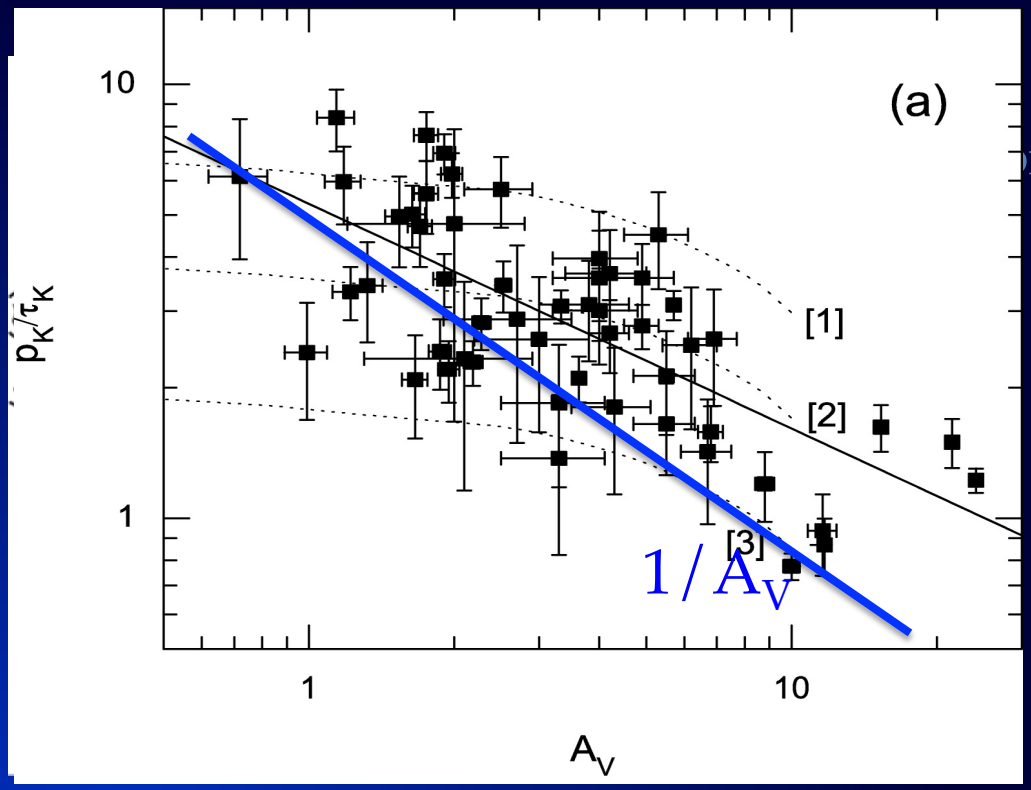

Whittet, Hough, Lazarian, Hoang (2008)

Reflection Nebula: IC 63

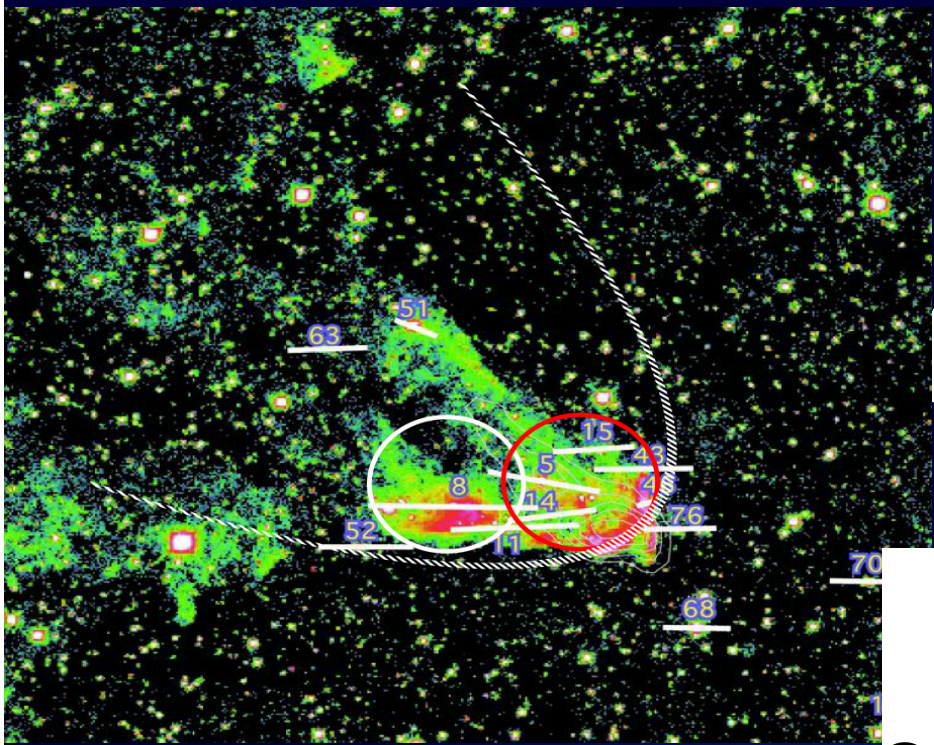

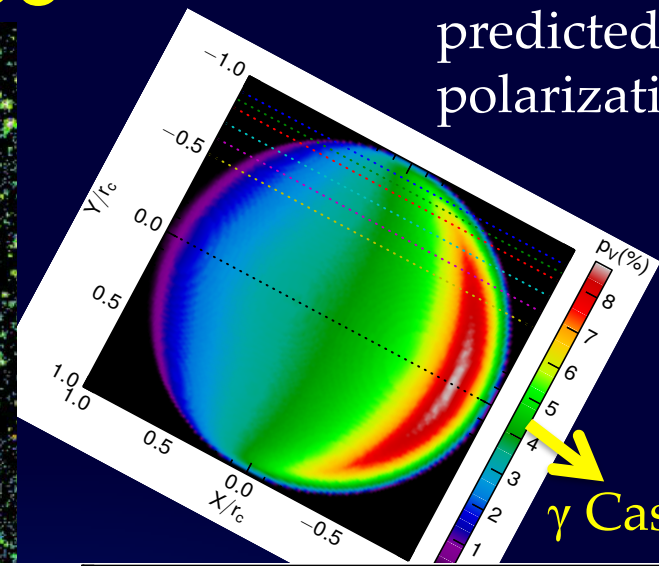

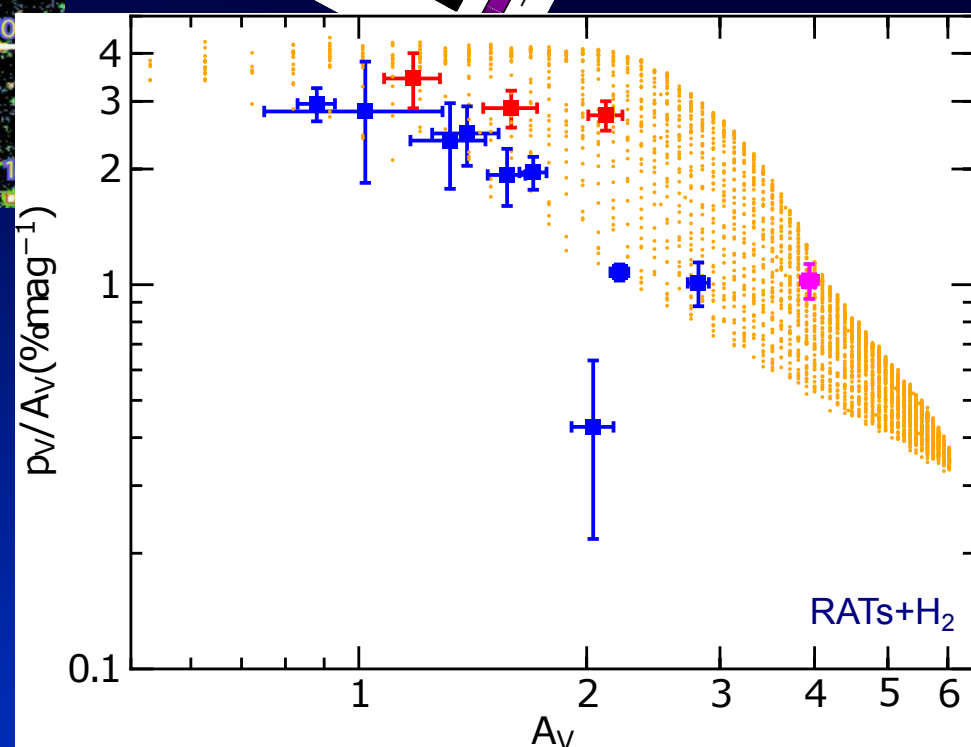

Hoang et al. 2014b

Polarized Emission from Molecular Cloud

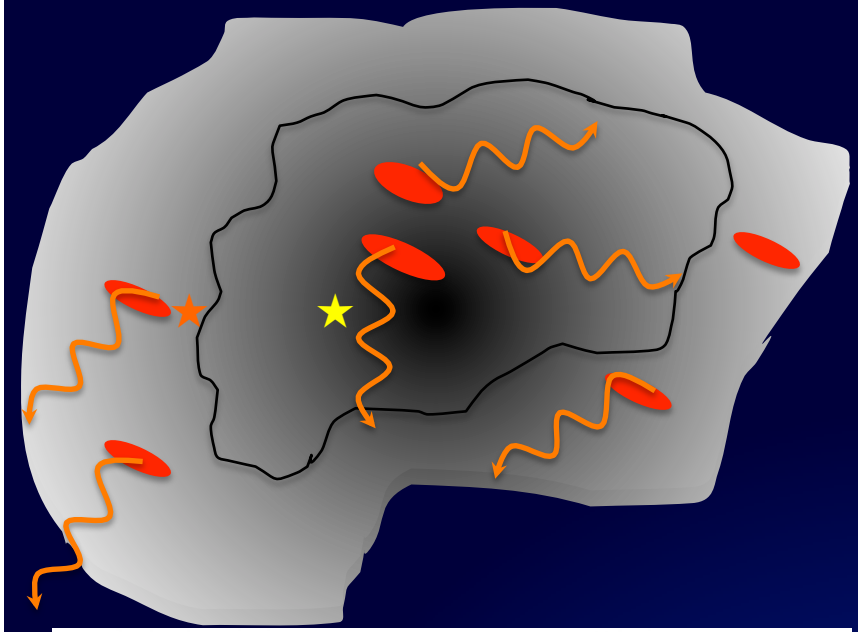

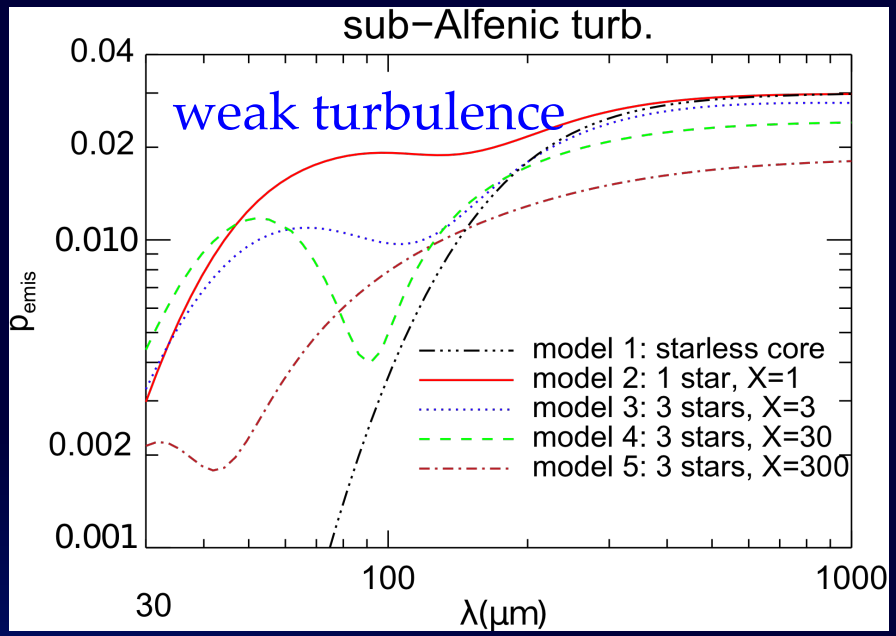

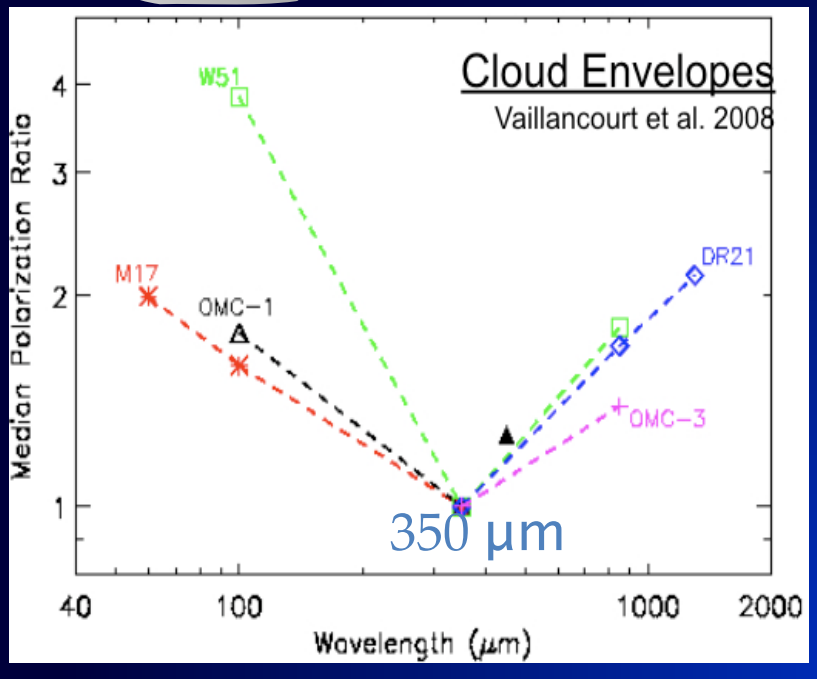

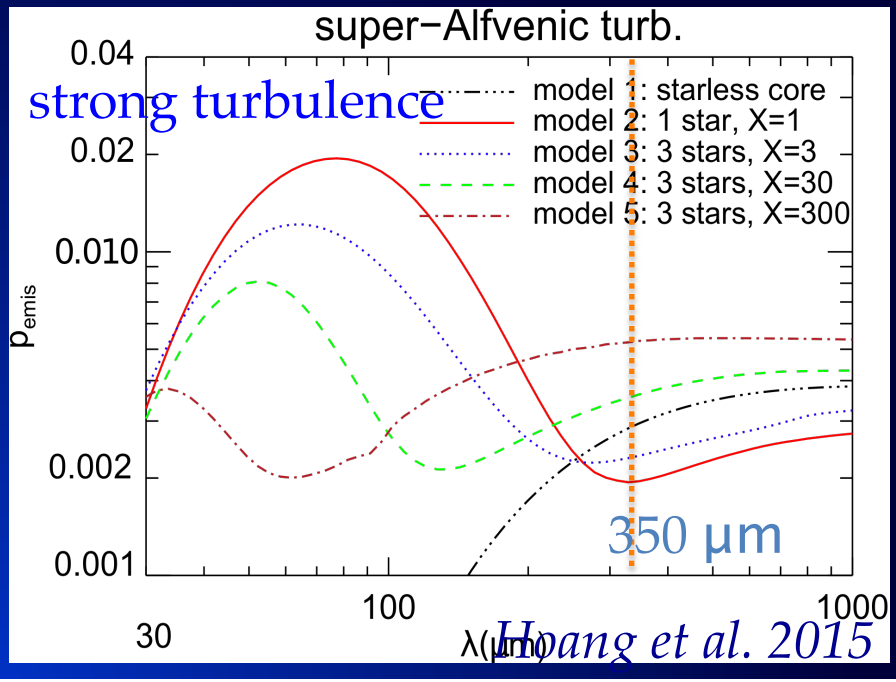

Hoang et al. 2015

Constraining Polarization of Spinning Dust from Starlight Polarization

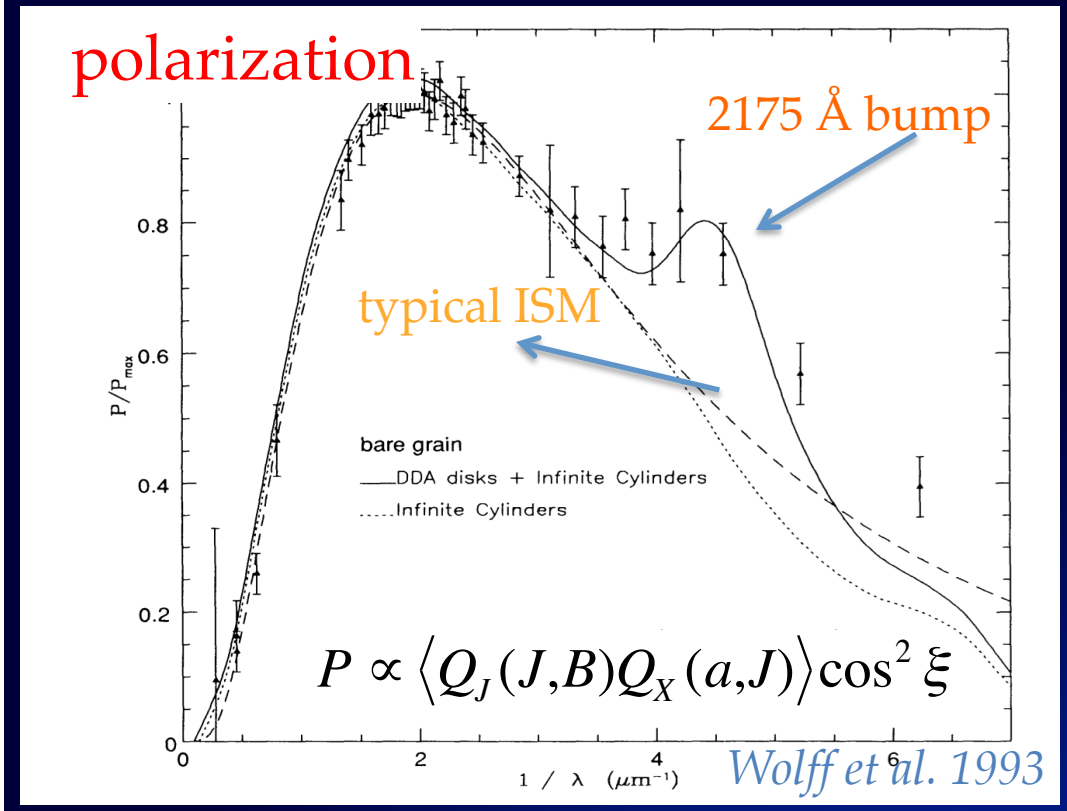

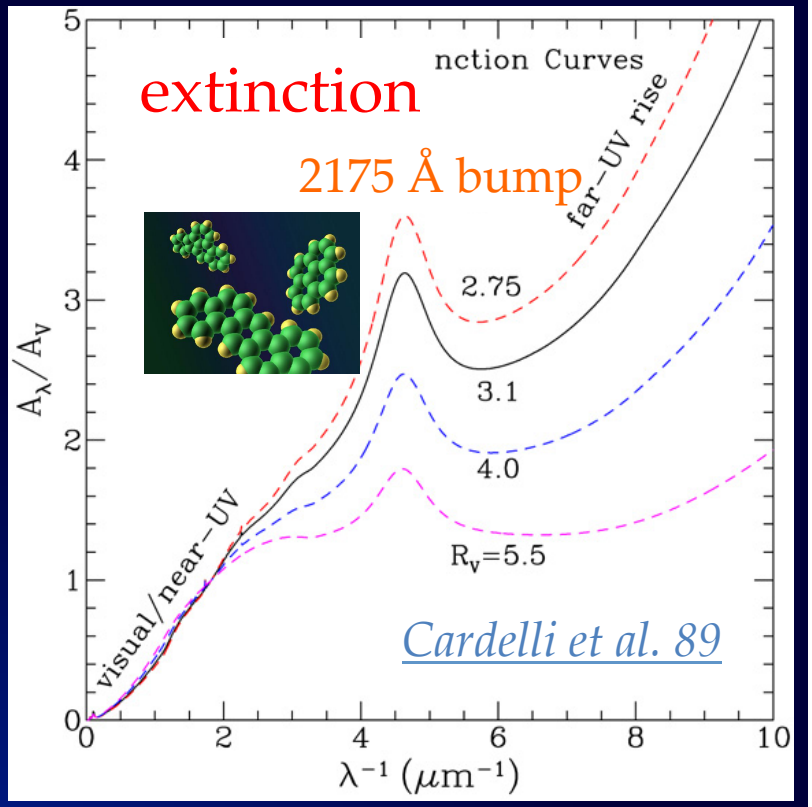

- PAHs produce 2175 Å (e.g., Draine 89)
- PAHs radiate spinnning dust emission
- How efficient are PAHs aligned?

Inversion Technique

- Adopting a model of dust: silicate & carbonaceous compositions
- Constructing a model (Kim & Martin 95, Draine & Fraisse 09):

$$A_{\mathrm{mod}}(\lambda_k) \propto \sum_{\mathrm{m=sil,carb}} \sum_{i=0}^{Na-1} n_d(a_i)\pi a_i^2 Q_{\mathrm{ext}}(a_i,\lambda_k)$$

$$P_{\mathrm{mod}}(\lambda_k) \propto \sum_{\mathrm{m=sil,carb}} \sum_{i=0}^{Na-1} f(a_i) n_d(a_i)\pi a_i^2 Q_{\mathrm{pol}}(a_i,\lambda_k)$$

Model parameters:

$n_d(a_i)$: grain size distribution

$f(a_i)$: alignment function

- Minimizing an objective function:

$$\chi^2_{\mathrm{ext}} = \sum_{k=0}^{N_\lambda-1} w_{\mathrm{ext}}\left[A_{\mathrm{mod}}(\lambda_k) - A_{\mathrm{obs}}(\lambda_k)\right]^2$$

$$\chi^2_{\mathrm{pol}} = \sum_{k=0}^{N_\lambda-1} w_{\mathrm{pol}}\left[P_{\mathrm{mod}}(\lambda_k) - P_{\mathrm{obs}}(\lambda_k)\right]^2$$

$$\chi^2 = \chi^2_{\mathrm{ext}} + \chi^2_{\mathrm{pol}} + \chi^2_{\mathrm{constraints}}$$

w_{ext}, w_{pol}: fitting weights

- Nonlinear Chi-square fitting: ~ N_a*N_λ free parameters
- Monte Carlo search method for global minimization

Hoang et al. 2014a

Best-fit Model Parameters

Degree of alignment

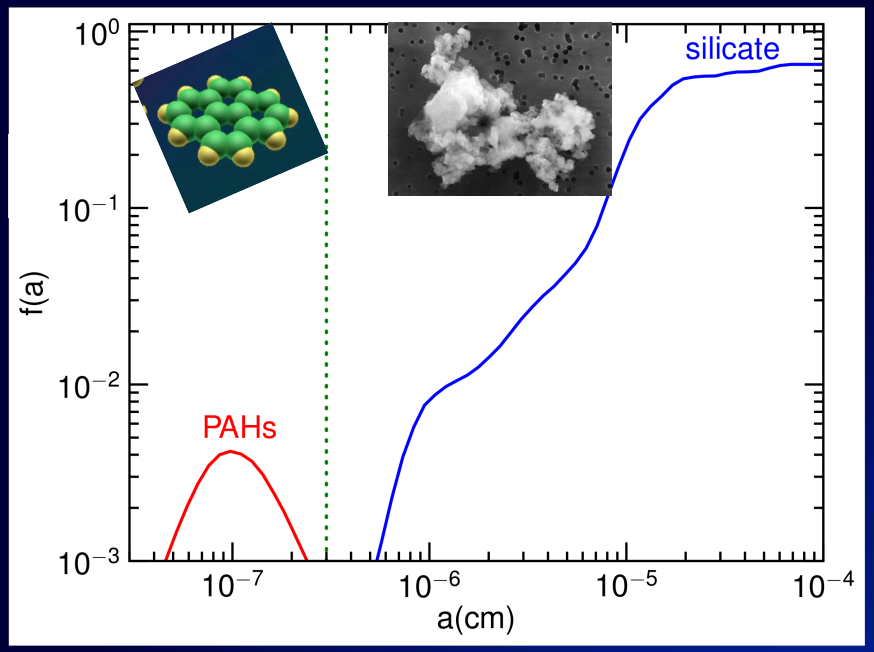

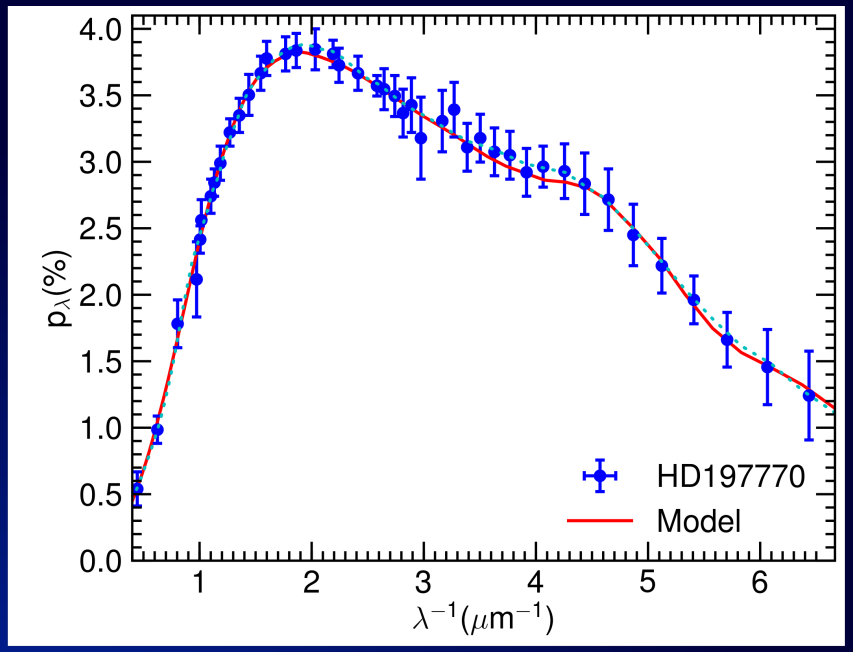

- PAHs are very weakly aligned
- Big silicates are efficiently aligned.

Maximum polarization of spinning dust is ~ 1.6 percent

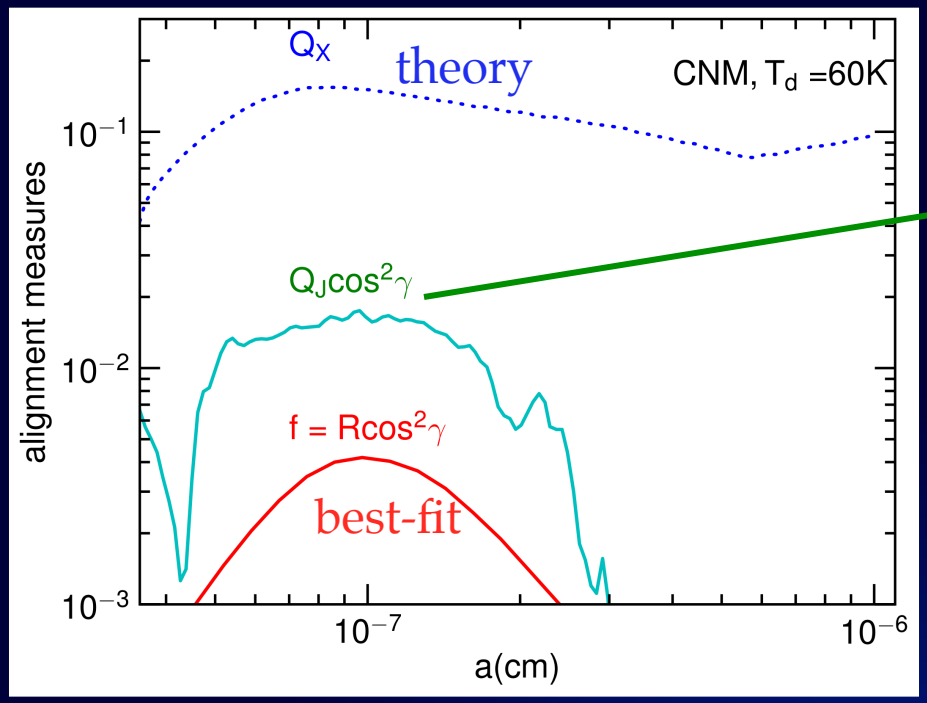

$$P \propto Q_J \cos^2 \gamma$$

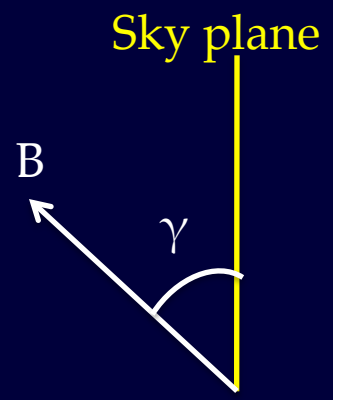

Polarization

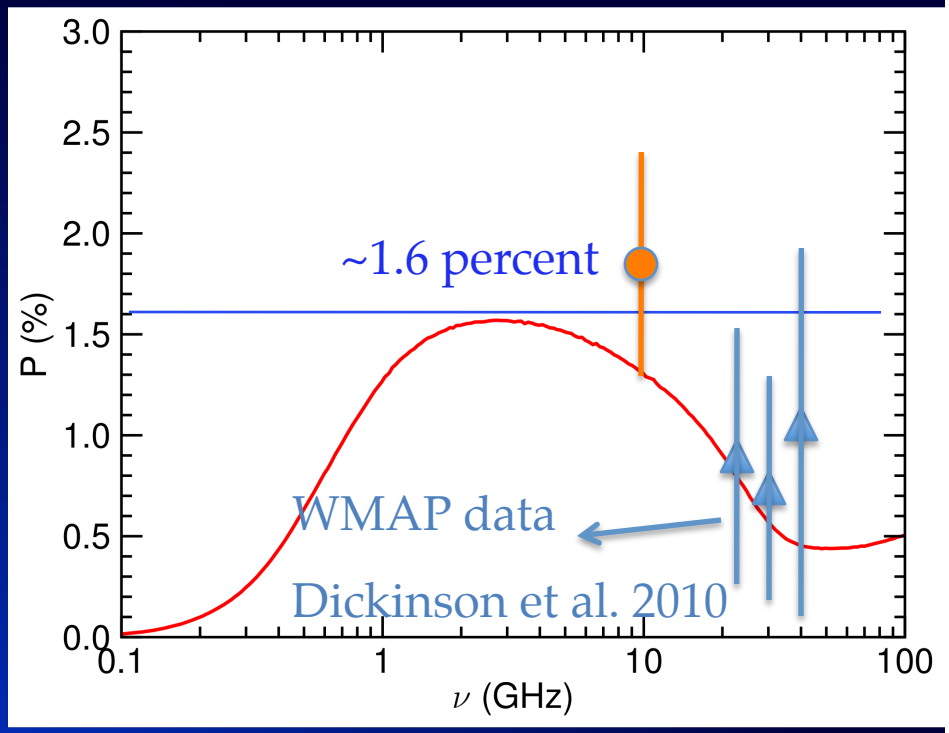

Future polarization data will test our predictions.

Hoang et al. 2013

Summary

1. Spinning dust emission becomes a new, accepted foreground.
2. A comprehensive model of spinning dust is established.
3. Spinning dust can be used to probe PAH physical parameters using observational data (e.g., Planck, coming SKA).
4. Spinning Dust Emission is very weakly polarized, but Thermal Dust Emission is highly polarized.
5. A predictive model of grain alignment is proposed and supported by numerous observations.
6. Combination of observations, theory and inversion technique is needed for precision modeling of dust polarization.

Thank you for your listening!